Development of an Appropriate Pedestrian Legform Impact Test Method which can be used for all Types of Vehicles including High Bumper Vehicles

- Development of a Simplified Upper Body Part (SUBP) FE Model -

Takahiro Isshiki, Atsuhiro Konosu, Yukou Takahashi

Abstract The current test methods using a legform impactor cannot appropriately evaluate the probability of pedestrian lower limb injuries when applied to vehicles with high bumpers (high-bumper vehicles) because of a lack of pedestrian upper body part/function in the impactors. Therefore, since 2010 we have been developing a legform impact test method that can evaluate the probability of pedestrian lower limb injuries when applied to any type of vehicle, including high-bumper vehicles.

In this research, as the second step of our study, we developed a finite element (FE) model of a Simplified Upper Body Part (SUBP) that can appropriately consider the influences of the upper body part of pedestrians.

First of all, because it can be considered that the influences of the upper body part of pedestrians are passed on to the lower limb via the hip joint located at the top of the lower limb, we analyzed the influence of differences in load conditions applied to the hip joint on the probability of lower limb injuries. As a result, we identified factors that significantly influence the probability of lower limb injuries.

Next, we developed a SUBP FE model considering the above-mentioned influential factors using the optimization method. As a result, we succeeded in developing a SUBP FE model that can appropriately consider the influences of the upper body part of pedestrians.

Keywords pedestrian protection test method, legform impactor, influences of the upper body part, computer simulation, optimization method

I. INTRODUCTION

The current test methods using a legform impactor simulating only a lower limb of a pedestrian, which are used under the current regulations, cannot appropriately evaluate the probability of lower limb injuries of pedestrians when applied to vehicles with high bumpers (high-bumper vehicles) [1-2]. The reason is that those legform impactors have neither a part corresponding to the upper body part of a pedestrian nor a mechanism to reproduce the influences of the upper body part. It means the upper body part of a pedestrian affects the probability of pedestrian lower limb injuries. Therefore, it is necessary to develop a pedestrian legform impact test method which can be applied to high-bumper vehicles.

In addition, the upper body part of a pedestrian also affects the probability of pedestrian lower limb injuries in collisions with low-medium-bumper vehicles. The test method using the flexible pedestrian legform impactor therefore attempts to compensate for the influences of the upper body part by setting the impact height 50 mm higher than that of an actual pedestrian, however, the compensation is not enough. The relative lower limb contact position to the vehicle differs from that of an actual pedestrian so initial loading conditions on the lower limb of the impactor differ from those of an actual pedestrian. Moreover, the impactor does not have the upper body parts of a pedestrian, therefore, it cannot evaluate femur loading conditions of an actual pedestrian appropriately. For these reasons, it is necessary to develop a pedestrian legform impact test method which is more appropriate than the current methods for low-medium-bumper vehicles.

We decided to develop a test method which can be applied to high-bumper vehicles as well as low-medium-bumper vehicles, considering the influences of the upper body part of a pedestrian, appropriately using the four steps shown in Figure 1.

*T. Isshiki (tel: +81-29-856-0885, email: tissiki@jari.or.jp) and A. Konosu - Japan Automobile Research Institute (JARI), Tsukuba, Japan.
Y. Takahashi - Japan Automobile Manufacturers Association, Inc. (JAMA), Tokyo, Japan.

In "Step-1: Analysis of Human Upper Body Part Influences", which was reported in an earlier study by the authors [3], the influences that the upper body part of pedestrians add to the probability of lower limb injuries in collisions with a high-bumper or low-medium-bumper vehicle were clarified using the CAE analysis method that uses a human Finite Element (FE) model. As a result, it was clarified that the influence of the upper body part tends to increase the probability of lower limb injuries in the case of collisions with high-bumper vehicles. In contrast, it was clarified that the influence of the upper body part tends to decrease the probability of lower limb injuries in the case of collisions with low-medium-bumper vehicles. In developing legform impact test methods, therefore, it is necessary to appropriately consider the influence of the upper body part of pedestrians, which differs depending on the shape of vehicle as described above.

In this study, "Step-2: Development of a Simplified Upper Body Part (SUBP) FE Model", we developed an FE model of a Simplified Upper Body Part (SUBP) that can appropriately consider the influence of the upper body part of pedestrians using the CAE analysis method.

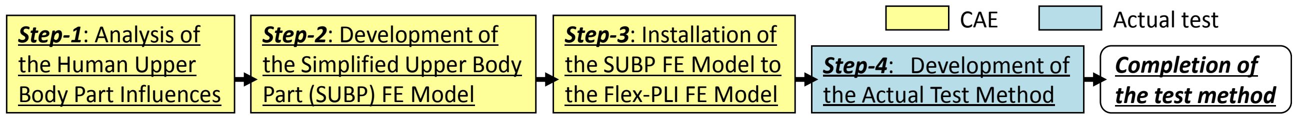

Fig. 1. Overall Flow of the Development of the Test Method

II. METHODS

Computer simulation Finite Element models

Figure 2 depicts the computer simulation FE models used in this study. In this study, we developed a "SUBP FE model" using a "simplified vehicle FE model", "human full body FE model", "simplified full body FE model", and "simplified pelvis FE model" with an optimization technique.

Regarding impact conditions between the simplified vehicle FE model and the other FE models, we used the same impact conditions between a vehicle and pedestrian targeted in the pedestrian safety global technical standard (impact direction: from the lateral side of a pedestrian, impact speed: 11.1 m/s, impact height: the sole of the foot of a pedestrian is 25 mm above the ground) [4].

Simplified vehicle FE model: The simplified vehicle FE model is composed of three parts: the Bonnet Leading Edge (BLE), Bumper (BP), and Spoiler (SP) (Figure 3). The BLE is composed of a deformable shell element that simulates the characteristics of cold rolled steel and the deformation characteristic of the BLE can be changed by varying the thickness of the shell element. The BP and SP are composed of a rigid shell element and a joint element. The joint element of BP and SP can be moved in only the longitudinal direction of the vehicle, and their movability characteristics are changed by varying the characteristic of the joint element (Appendix Figure A-1). Two different levels were set for the deformation characteristic of the BLE. Three different levels were set for the movability characteristic of the BP and SP, respectively (Appendix Table A-I). The vehicle shape can be changed by varying the positions of BLE, BP and SP (Appendix Figure A-2). Regarding parameters of vehicle shape, three different levels were set for the positioning of BLE, BP and SP, respectively, by referring to the vehicle shape corridor provided by the International Harmonized Research Activity (IHRA) [5] (Appendix Table A-I). By putting the above-mentioned levels in the L18 orthogonal table of the experiment design, we prepared simplified vehicle FE models for a total of 36 vehicle types, including a simplified high-bumper vehicle FE model for 18 vehicle types (SUV01 to 18) and a simplified low-medium-bumper vehicle FE model for 18 vehicle types (Sedan 01 to 18) (Appendix Table A-II and Figure A-3).

Human full body FE model: The human full body FE model is verified in detail using Post Mortem Human Subject (PMHS) component levels and full body levels test data; it therefore has high biofidelity to the human body [6-9]. For the setting of the walking posture of the human full body FE model, a gait stance where the lower limb on the side of the initial collision with the vehicle is vertical and the lower limb on the opposite side is 20 degrees ahead of the pedestrian (Figure 4) was adopted. In this gait stance, the total weight of the human full body FE model is applied to the lower limb on the side of the initial collision with the vehicle. This gait stance is considered as the severest load condition on the lower limb on the side of the initial collision with the vehicle, and the regulations for pedestrian lower limb protection used in Japan, Europe and the UN also assume the same load condition. A total of eight measurement items for evaluating the probability of injuries of the human full body FE model (hereinafter “injury evaluation items”) were measured, i.e. the bending moment of the femur (Femur-1 to 3), the elongation of the medial collateral ligament of the knee (MCL) and the bending moment of the tibia (Tibia-1 to 4) (Figure 4). The elongations of the anterior cruciate ligament (ACL) and posterior cruciate ligament (PCL) of the knee were not adopted in this study because cases of isolated injury to the ACL or PCL are rare under a car impact situation from the lateral side of a pedestrian [10]; in other words, they are commonly accompanied by injury to the MCL.

Simplified full body FE model: The simplified full body FE model is a model where all the parts of the human full body FE model, other than the lower limb on the side of the initial collision with the vehicle, are replaced with four rigid body elements and five joint elements. The four rigid body elements reproduce the mass and the moment of inertia of the head + chest + abdomen + arms; pelvis; thigh on the opposite side of the initial collision with the vehicle; and leg on the opposite side of the initial collision with the vehicle of the human full body FE model. The five joint elements connect the above rigid body elements. It can be considered that the influences of the upper body part of pedestrians are passed on to the lower limb via the hip joint. The simplified full body FE model therefore facilitates measurement of the load (moment and force) conditions applied to the hip joint on the side of the initial collision with the vehicle to clarify important load conditions that should be considered in developing the SUBP FE model.

Simplified pelvis FE model: The simplified pelvis FE model is a model where all the parts of the simplified full body FE model, other than the lower limb on the side of the initial collision with the vehicle and the rigid body element representing the pelvis, are removed from the simplified full body FE model.

SUBP FE model: The SUBP FE model is a model where the parameters of each specification for the simplified pelvis FE model are optimized, enabling us to appropriately consider the influences that the upper body part of pedestrians add to the probability of lower limb injuries.

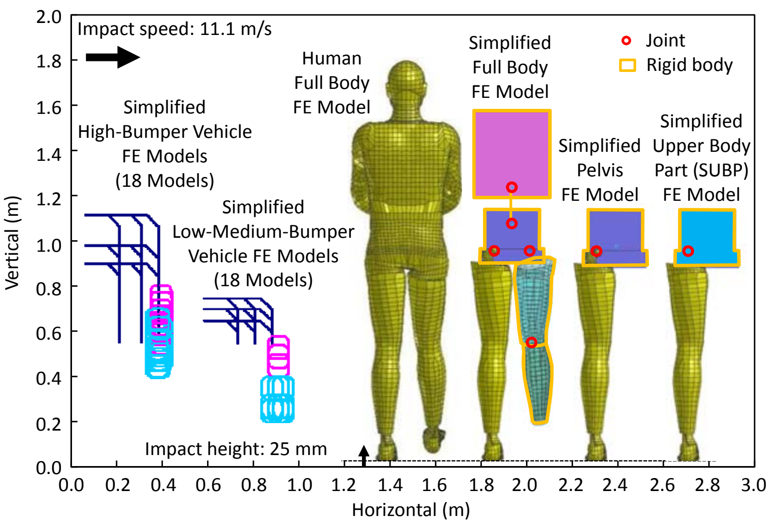

Fig. 2. Computer Simulation FE Models used in this Study

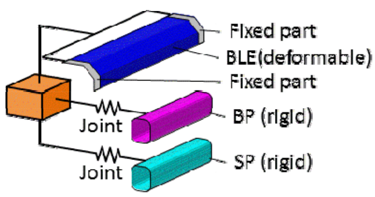

Fig. 3. Configuration of the Simplified Vehicle FE Model

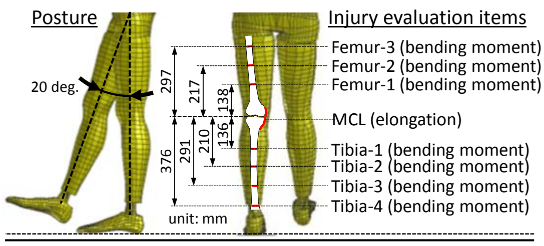

Fig. 4. Posture and Injury Evaluations Items for the Human Full Body FE Model

Flow of this study

In this study, we developed the SUBP FE model using the steps from Step-2.1 to Step-2.4 shown in Figure 5.

Step-2: Development of the Simplified Upper Body Part (SUBP) FE Model

- **Step-2.1:** Development of the Simplified Full Body FE Model (Base Model)
- **Step-2.2:** Define Acceptance Levels
- **Step-2.3:** Simplification of the Base Model
- **Step-2.4:** Optimization of the Simplified Pelvis Model
  - **Step-2.4(a):** Investigate important boundary conditions around the hip joint for the optimization process
  - **Step-2.4(b):** Select Optimization Parameters
  - **Step-2.4(c):** Set Variation Level for each Optimization Parameter
  - **Step-2.4(d):** Optimization
- **Completion of the SUBP FE model**

Fig. 5. Flow of this Study

Step-2.1: Development of the Simplified Full Body FE Model (Base Model)

As the first step of development of the SUBP FE model, we developed the simplified full body FE model. The simplified full body FE model was developed by replacing all the parts of the human full body FE model, other than the lower limb on the side of the initial collision with the vehicle, with the four rigid body elements and five joint elements. Consequently, it is estimated that the model correlates well with the human full body FE model. Therefore, the validity of the simplified full body FE model was simply confirmed by comparing the correlation analysis results regarding MCL and tibia outputs (the variation of correlation, the coefficient of correlation and the slope of the regression line) of the simplified full body FE model and human full body FE model against the simplified vehicle FE models for all 36 vehicle types with those of the flexible pedestrian legform impactor FE model and the human full body FE model [11] that is conducted in development activities of the draft amendments of the pedestrian safety global technical regulation.

Step-2.2: Define Acceptance Levels

In the following steps, we developed the SUBP FE model by modifying the simplified full body FE model developed in Step-2.1. The SUBP FE model and interim model in the development was constructed quite differently from the simplified full body FE model. We therefore set the acceptance level of the equivalency with the human full body FE model in order to evaluate the appropriateness in more detail.

The acceptance level was based on correlation analysis of the simplified full body FE model and human full body FE model against the simplified vehicle FE models for all 36 vehicle types in Step-2.1 with regard to (1) standard deviation, (2) correlation coefficient, (3) slope of the regression line, and (4) timing of occurrence of the maximum value of all of the injury evaluation items (Femur, Tibia, and MCL).

Step-2.3: Simplification of the Base Model

We developed the simplified pelvis FE model by removing all parts of the simplified full body FE model other than the lower limb on the side of the initial collision with the vehicle and the rigid body element representing the pelvis. Its appropriateness was evaluated using the quantitative acceptance level determined in Step-2.2.

Step-2.4: Optimization of the Simplified Pelvis FE Model

We optimized the simplified pelvis FE model that was developed in Step-2.3, as the final phase of development of the SUBP FE model. Step-2.4 was implemented based on following the steps (a) to (d).

Step-2.4(a): Investigate important boundary conditions around the hip joint for the optimization process

We implemented analysis of the degree of influence of the load conditions at the hip joint on the output values of injury evaluation items because the differences of the output values of injury evaluation items between the simplified pelvis FE model and human full body FE model can be caused by the differences in load conditions at the hip joint. Among the load conditions for the hip joint of the simplified full body FE model, we selected the conditions of the load in the three directions that may influence the output of injury evaluation items (Moment around X-axis: Mx, Force along Y-axis: Fy, and Force along Z-axis: Fz) (Figure 6) as the object of analysis. By giving the moment or force occurring at the hip joint of the simplified full body FE model, which is used as the base model of this study, to the hip joint of the simplified pelvis model as an enforced load while varying it within the range from 0%, 50%, 75%, 125%, 150%, to 200% (Figure 7), we investigated the degree of influence on the output values of injury evaluation items.

The conditions of the load in the three directions that are considered not to influence injury evaluation items (Moment around Y-axis: My, Moment around Z-axis: Mz, and Force along X-axis: Fx) were not adopted as the object of this analysis. Therefore, enforced rotation and enforced displacement were applied to the hip joint of the simplified pelvis FE model to maintain the consistency of the conditions of the load (My, Mz, and Fx) with that of the simplified full body FE model. Furthermore, the deformation of the vehicle due to the contact with the upper body part was not adopted as the object of this analysis because of clarification of hip joint load influences simply using the above varying hip joint loading conditions. Therefore, the same deformation of the vehicle was reconstructed by applying enforced displacement and enforced rotation to the pelvis part of the simplified pelvis FE model.

A total of three vehicle types were used for the simplified vehicle FE models used in this analysis, i.e., (1) SUV01, which has an ordinary SUV shape among the simplified high-bumper vehicle FE models, (2) Sedan16, which has a relatively high vehicle-front shape among the simplified low-medium-bumper vehicle FE models, and (3) Sedan01, which has a relatively low vehicle-front shape among the simplified low-medium-bumper vehicle FE models (Figure 8).

From the results of this analysis, we clarified the load conditions on the hip joint that have relatively large influences on the output values of injury evaluation items and then utilized them as important load conditions in the subsequent steps.

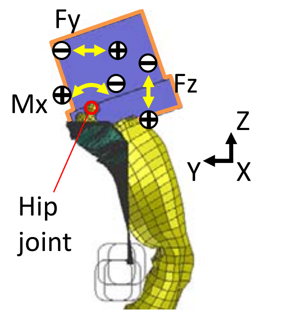

Fig. 6. Directions of the Enforced Moment and Load Applied to the Hip Joint

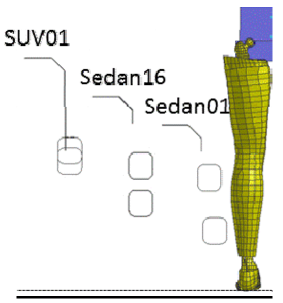

Fig. 8. Simplified Vehicle FE Models used in Step-2.4(a)

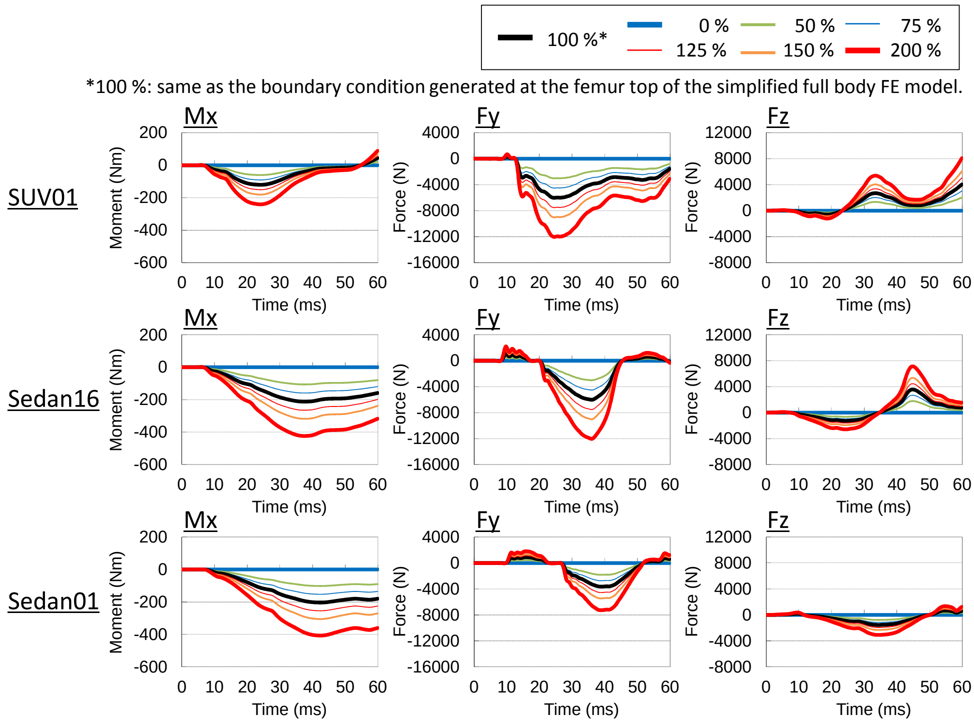

Fig. 7. Waveforms with Time of the Enforced Moment and Force Applied to the Hip Joint used in Step-2.4(a)

Step-2.4(b): Select Optimization Parameters

We clarified the parameters of each specification for the simplified pelvis FE model that may have an influence on the important load conditions of the hip joint as clarified in Step-2.4(a) and on injury evaluation items, by implementing sensitivity analysis on the parameters of each specification to extract the parameters for optimization analysis.

In this analysis, we selected the parameters concerning (1) physical characteristics of the pelvis, (2) contact conditions between the pelvis and vehicle, and (3) characteristics of the hip joint (Appendix Figure A-4), which are considered to influence the load conditions of the hip joint and injury evaluation items. By varying the values quantitatively, we checked their sensitivity to the load conditions of the hip joint and injury evaluation items.

We used a total of two vehicle types with largely different vehicle-front shapes, i.e., “SUV01”, which has an ordinary SUV shape among the simplified high-bumper vehicle FE models, and “Sedan01”, which is a vehicle having a relatively low vehicle-front shape among the simplified low-medium-bumper vehicle FE models.

From the results of this analysis, we extracted those parameters that have high sensitivity to the load conditions of the hip joint and injury evaluation items in the case of the collision with either SUV01 or Sedan01 or both to use them as the parameters for optimizing the specifications for the simplified pelvis FE model thereafter.

Step-2.4(c): Set Variation Level for Each Optimization Parameter

We set the variation levels for each parameter, extracted in Step-2.4(b), to optimize the simplified pelvis FE model. When setting variation levels for each parameter, we used the proviso that (1) the differences of the femur bending moment waveform with the simplified full body FE model are insignificant (the peak value and its timing do not differ from the simplified full body FE model) and (2) the trend of the change in the maximum value of injury evaluation items is linear.

Step-2.4(d): Optimization

We implemented optimization of the simplified pelvis FE model using the parameters extracted in Step-2.4(b) and the variation levels set in Step-2.4(c).

Here, optimization was implemented using the "Taguchi Method" and based on the following flow [12].

Optimization flow:

・ Assign the parameters and variation levels to the L36 orthogonal table of the experimental design to prepare simplified pelvis FE models of 36 specifications (Model01 to Model36) (Appendix Table A-III).

・ Perform collision analysis for the simplified pelvis FE models of 36 specifications against a total of two vehicle types with largely different vehicle-front shapes, i.e., "SUV01", which has an ordinary SUV shape among the simplified high-bumper vehicle FE models and "Sedan01", which is a vehicle having a relatively low vehicle-front shape among the simplified low-medium-bumper vehicle FE models.

・ Calculate the integrated values (+ side and – side, respectively) of the differences of the femur bending moment (Femur-1 to 3) waveform with the human full body FE model (Appendix Figure A-5).

・ Calculate the Signal Noise ratio (SN ratio) using the calculated integrated values according to the equations (1) and (2).

$$\text{SN ratio} = -10\log V_e \quad (1)$$

$$V_e = \frac{1}{n-1}\sum\left(y-\bar{y}\right)^2 \quad (2)$$

where, V_e: unbiased variance of the integrated values,
n: number of the integrated values, y: the integrated values.

・ Select the combination of the levels of each parameter that maximize the SN ratio: Larger SN ratio means that the differences of the femur bending moment waveform with the human full body FE model (integrated values) are more constant.

・ Construct a SUBP FE model that reflects the selected levels.

Lastly, we evaluated the appropriateness of the SUBP FE model using the quantitative acceptance level determined in Step-2.2.

III. RESULTS

Step-2.1: Development of the Simplified Full Body FE Model (Base Model)

Figure 9 shows the results of correlation analysis of the simplified full body FE model and human full body FE model that were developed in this step against the simplified vehicle FE models for all 36 vehicle types. From this figure, the simplified full body FE model is superior to the flexible pedestrian legform impactor FE model in the following ways: It has a smaller variation of correlation and a higher coefficient of correlation, and the slope of the regression line is closer to 1. The validity of the simplified full body FE model was thus confirmed.

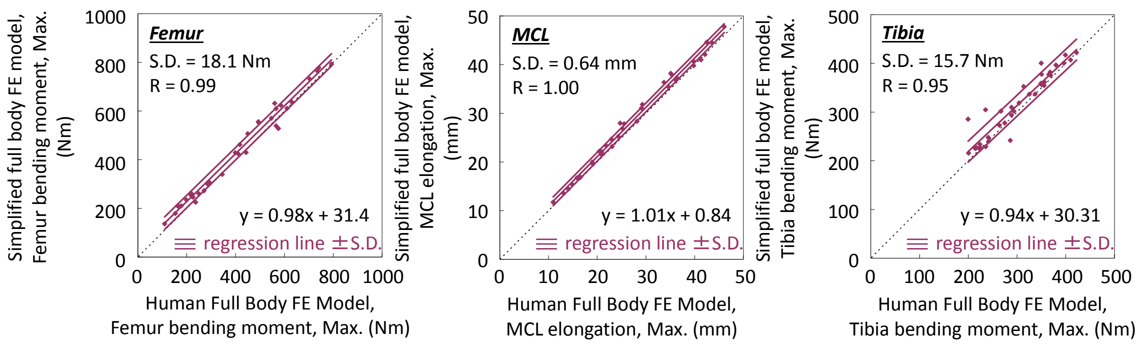

Fig. 9. Results of Correlation Analysis of the Simplified Full Body FE Model and Human Full Body FE Model

Step-2.2: Define Acceptance Levels

Table I shows the quantitative acceptance level for the equivalency with the human full body FE model, which was determined in this step, together with the quantitative correlation analysis results on the simplified full body FE model. The quantitative acceptance level was set based on the correlation analysis results regarding the simplified full body FE model and human full body FE model against the simplified vehicle FE models for all 36 vehicle types. The table indicates the simplified full body FE model falls in the range of the acceptance level.

TABLE I
THE QUANTITATIVE ACCEPTANCE LEVEL FOR EQUIVALENCY WITH THE HUMAN FULL BODY FE MODEL AND THE RESULTS ON THE SIMPLIFIED FULL BODY FE MODEL

Item		Acceptance Level	Simplified Full Body FE Model
Femur	Standard Deviation (S.D.)	≤ 23 Nm	18.1 Nm
	Correlation Coefficient (R)	≥ 0.8	0.99
	slope of Regression Line	≥ 0.7 and ≤ 1.3	0.98
	Timing of Absolute Maximum Values	Within +/- 10 ms difference: more than 75 %	100.00%
MCL	Standard Deviation (S.D.)	≤ 1.5 mm	0.64 mm
	Correlation Coefficient (R)	≥ 0.8	1
	slope of Regression Line	≥ 0.7 and ≤ 1.3	1.01
	Timing of Absolute Maximum Values	Within +/- 10 ms difference: more than 75 %	100.00%
Tibia	Standard Deviation (S.D.)	≤ 23 Nm	15.7 Nm
	Correlation Coefficient (R)	≥ 0.8	0.95
	slope of Regression Line	≥ 0.7 and ≤ 1.3	0.94
	Timing of Absolute Maximum Values	Within +/- 10 ms difference: more than 75 %	94.40%

Step-2.3: Simplification of the Base Model

Figure 10 shows the correlation analysis results of the simplified pelvis FE model and the human full body FE model against the simplified vehicle FE models for all 36 vehicle types. From this figure, it can be seen that the simplified pelvis FE model does not satisfy the quantitative acceptance level for the equivalency to the human full body FE model in terms of the standard deviation of the maximum value of the femur (Quantitative acceptance of maximum value of the femur: S.D. ≤ 23 Nm). Therefore, we decided to implement optimization of each specification of the simplified pelvis FE model thereafter.

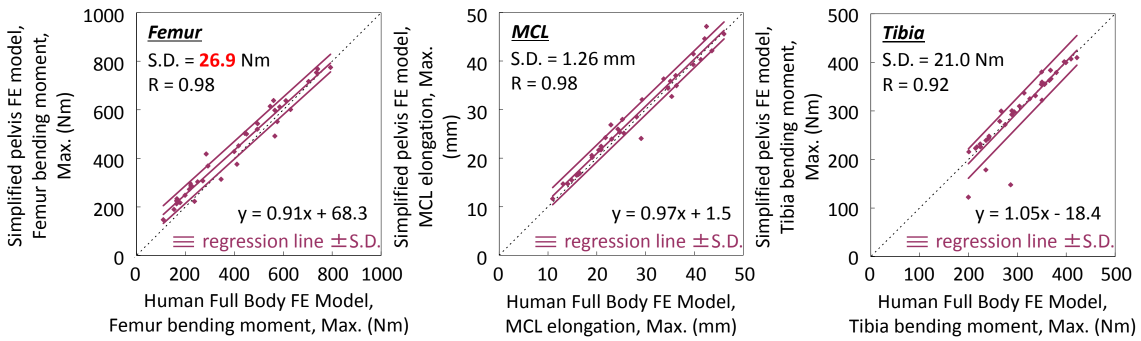

Fig. 10. Results of Correlation Analysis of the Simplified Pelvis FE Model and the Human Full Body FE Model

Step-2.4(a): Investigate important boundary conditions around the hip joint for the optimization process

Figure 11 shows the analysis results for the degree of influence that the load conditions to the hip joint (Mx, Fy, and Fz) passes on to the output values of injury evaluation items. In this figure, a larger absolute value of the slope of the regression line indicates a larger degree of influence on the output values of injury evaluation items. From this figure, the following facts were revealed.

- In the case of collision with "SUV01" and "Sedan16", the influence of Fy is significant with negligible influences of Mx and Fz.
- In the case of collision with "Sedan01", the influence of Fy is the largest followed by large influences of Mx and Fz.

This suggests that the load on the hip joint that is applied in the vehicle longitudinal direction, Fy, has a large influence on the output of injury evaluation items in the case of a vehicle that has a relatively high vehicle-front shape (e.g., SUV01 and Sedan16) and, on the other hand, other elements (Mx, Fz) also have an influence in the case of vehicles that have a relatively low vehicle-front shape (e.g., Sedan01). Therefore, when we developed the SUBP FE model, we focused on Fy as the important load condition on the hip joint for those vehicles that have a high vehicle-front shape and focused on Mx, Fy, and Fz as the important load conditions on the hip joint for those vehicles that have a low vehicle-front shape.

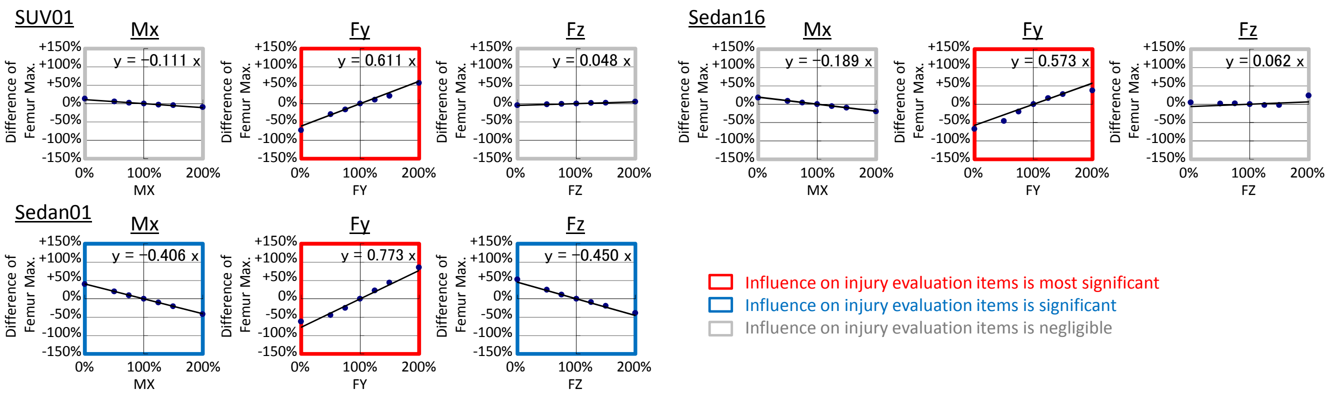

Fig. 11. Analysis Results of the Degree of Influences

Step-2.4(b): Select Optimization Parameters

Figure 12 shows an example of results of sensitivity analysis for parameters of the specifications for the simplified pelvis FE model to load conditions on the hip joint and the output values of injury evaluation items. This figure shows the results of sensitivity analysis where mass was changed. When mass was changed, sensitivity to the femur output is large, in collisions with SUV01. Therefore, we decided to use mass as one of the parameters of the specifications for optimizing the simplified pelvis FE model, expecting to improve the femur output of that model.

Similarly, we implemented sensitivity analysis on all parameters concerning (1) physical characteristics of the pelvis, (2) contact conditions between the pelvis and vehicle, and (3) characteristics of the hip joint (Appendix Figure A-6 to Figure A-27). As a result, we successfully extracted a total of 12 parameters with sensitivity for optimization as shown in Table II. Thereafter, we decided to implement optimization of the simplified pelvis FE model using these 12 extracted parameters.

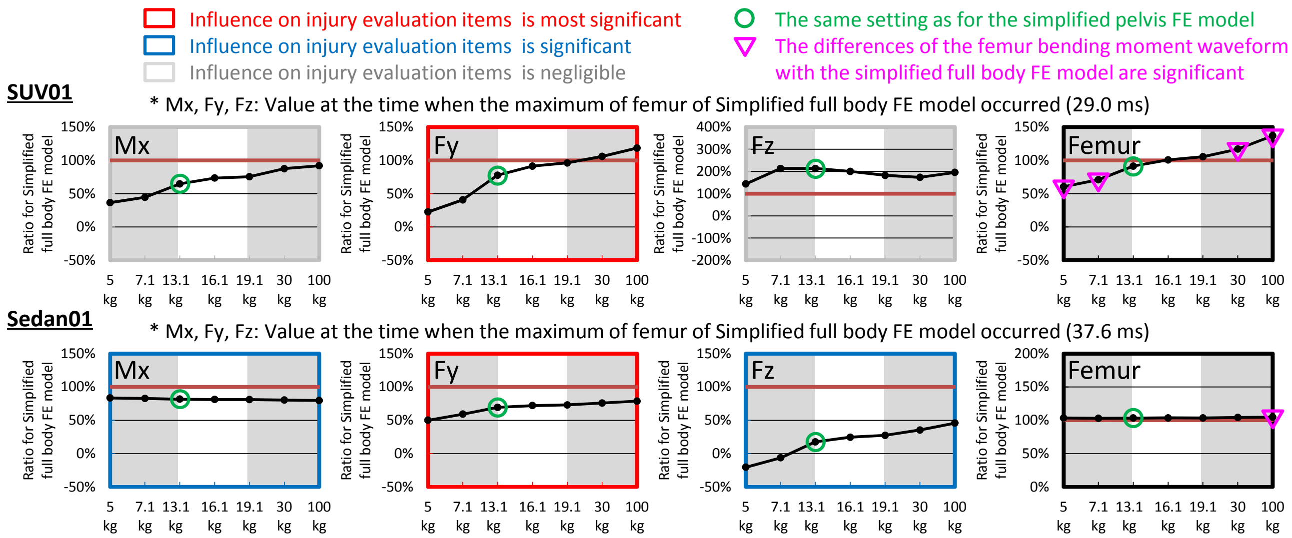

Fig. 12. Results of Sensitivity Analysis on the Simplified Pelvis FE Model (examples for Mass)

TABLE II

INFLUENCES ON IMPORTANT LOAD CONDITIONS ON THE HIP JOINT AND THE OUTPUT VALUES OF INJURY EVALUATION ITEMS

Item		Symbol	Influence (effectiveness for optimization)
(1)-1. Mass		Mass	**YES (effective)**
(1)-2. Moment of inertia	X-axis	Ix	**YES (effective)**
	Y-axis	Iy	NO (not effective)

	Z-axis	Iz	NO (not effective)
(1)-3. Coordinate of center of gravity	X-axis	COGx	NO (not effective)
	Y-axis	COGy	**YES (effective)**
	Z-axis	COGz	**YES (effective)**
(2)-1. Location Offset		Offset	**YES (effective)**
(2)-2. Stiffness/Shape		Stiffness/Shape	NO (not effective) or can be altered by (2)-1
(3)-1-a. Rotation-X	allowance* -	Rx(-)a	**YES (effective)**
	slope -	Rx(-)s	**YES (effective)**
	slope +	Rx(+)s	NO (not effective)
(3)-1-b. Rotation-Y	slope +/-	Ry(+/-)s	NO (not effective)
(3)-1-c. Rotation-Z	slope +/-	Rz(+/-)s	NO (not effective)
(3)-2-a. Displacement-X	slope +/-	Dx(+/-)s	NO (not effective)
(3)-2-b. Displacement-Y	allowance* -	Dy(-)a	**YES (effective)**
	slope -	Dy(-)s	**YES (effective)**
	slope +	Dy(+)s	NO (not effective)
(3)-2-c. Displacement-Z	allowance* -	Dz(-)a	**YES (effective)**
	slope -	Dz(-)s	**YES (effective)**
	slope +	Dz(+)s	**YES (effective)**

* Allowance: The range of free rotation or free displacement of the hip joint.

Step-2.4(c): Set Variation Level for Each Optimization Parameter

Table III shows the levels for each parameter determined in this step. Each level was set with the proviso that (1) the differences of the femur bending moment waveform with the simplified full body FE model are insignificant and (2) the trend of the change in the maximum value of injury evaluation items is linear on the basis of the sensitivity analysis results in Step-2.3(c) (Figure 12 and Appendix Figure A-6 to Figure A-27). Thereafter, we decided to implement optimization of the simplified pelvis FE model using each parameter and each variation level set in the above step.

TABLE III
PARAMETERS AND VARIATION LEVLS FOR OPTIMZATION ANALYSIS

Parameter		Symbol	Level		
			Level 1	Level 2	Level 3
Mass		Mass	13.1 kg	16.1 kg	19.1 kg
Moment of inertia	X-axis	Ix	x1	x2	x5
Coordinate of center of gravity	Y-axis	COGy	L* 100 mm	0 mm	R* 200 mm
	Z-axis	COGz	U** 50 mm	0 mm	D** 23 mm***
Location Offset		Offset	0 mm	-20 mm	-40 mm
Rotation-X	allowance -	Rx(-)a	0 deg.	10 deg.	20 deg.
	slope -	Rx(-)s	x0.1	x1	x1.5
Displacement-Y	allowance -	Dy(-)a	0 mm	5 mm	10 mm
	slope -	Dy(-)s	x0.5	x1	x100
Displacement-Z	allowance -	Dz(-)a	0 mm	25 mm	50 mm
	slope -	Dz(-)s	x0.5	x1	x2
	slope +	Dz(+)s	x0.1	x1	x100

* L (Left): Left hand side direction from the pedestrian view, R (Right): Right hand side direction from the pedestrian view.
** U (Up): The center of gravity moves upward along the vertical direction, D (Down): The center of gravity moves downward along the vertical direction.
The same setting as for the simplified pelvis FE model.

Step-2.4(d): Optimization

Figure 13 shows the graphs of factorial effects of the SN ratio calculated from the analysis results on the simplified pelvis models for 36 specifications. From this figure, we selected a combination of the levels that maximizes the SN ratio of each parameter to develop the SUBP FE model.

Figure 14 shows the correlation analysis results of the developed SUBP FE model and the human full body FE model against the simplified vehicle FE models for all 36 vehicle types. From this figure, it can be observed that the SUBP FE model has a high correlation with the human full body FE model.

Table IV shows the judgment result as to the equivalency of the SUBP FE model to the human full body FE model together with the results on the simplified full body FE model and simplified pelvis FE model. From this table, it can be verified that the SUBP FE model satisfies all the quantitative acceptance levels concerning the equivalency to the human full body FE model.

In addition, Appendix Figure A-28 and Figure A-29 show the waveforms concerning the injury evaluation items of the SUBP FE model and the human full body FE model for references. From this figure, it can be seen that the waveforms of the SUBP FE model and the human full body FE model are equivalent to each other.

From the above results in this study, it can be stated that we successfully developed the SUBP FE model, which can appropriately consider the influence of the upper body part.

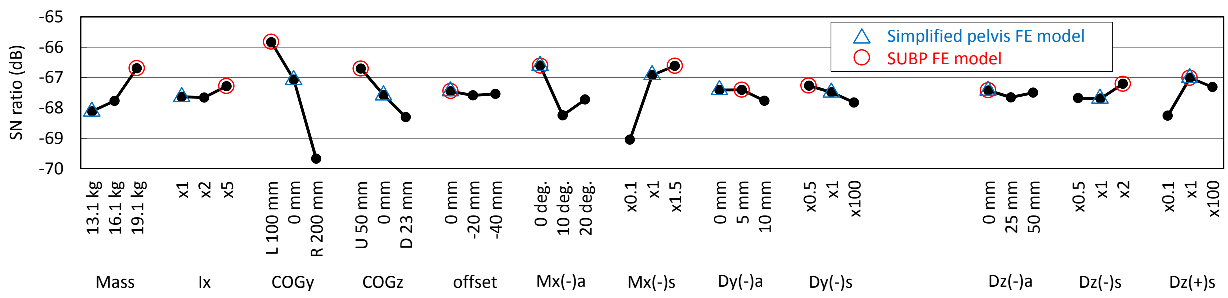

Fig. 13. Graphs of Factorial Effects of SN Ratio

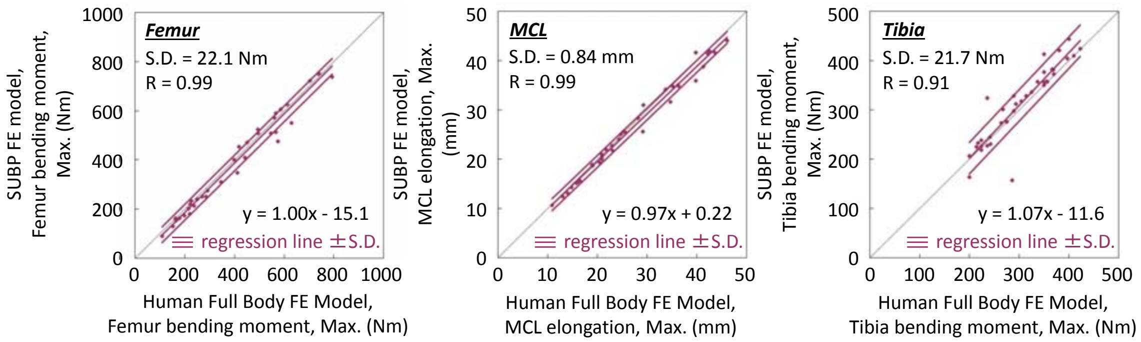

Fig. 14. Correlation Analysis Results of the SUBP FE Model and the Human Full Body FE Model

TABLE IV
QUANTITATIVE ACCEPTANCE LEVEL CONCERNING THE EQUIVALENCY TO THE HUMAN FULL BODY FE MODEL AND THE RESULTS ON THE SIMPLIFIED FULL BODY FE MODEL, SIMPLIFIED PELVIS FE MODEL AND SUBP FE MODEL

Item		Acceptance Level	Simplified full body FE model	Simplified pelvis FE model	SUBP FE model
Femur	Standard Deviation (S.D.)	≤ 23 Nm	18.1 Nm	**26.9 Nm**	22.1 Nm
	Correlation Coefficient (R)	≥ 0.8	0.99	0.98	0.99
	slope of Regression Line	≥ 0.7 and ≤ 1.3	0.98	0.91	1
	Timing of Absolute Maximum Values	Within +/- 10 ms difference: more than 75 %	100.00%	83.30%	94.40%
MCL	Standard Deviation (S.D.)	≤ 1.5 mm	0.64 mm	1.26 mm	0.84 mm
	Correlation Coefficient (R)	≥ 0.8	1	0.98	0.99
	slope of Regression Line	≥ 0.7 and ≤ 1.3	1.01	0.97	0.97
	Timing of Absolute Maximum Values	Within +/- 10 ms difference: more than 75 %	100.00%	97.20%	100.00%
Tibia	Standard Deviation (S.D.)	≤ 23 Nm	15.7 Nm	21.0 Nm	21.7 Nm
	Correlation Coefficient (R)	≥ 0.8	0.95	0.92	0.91
	slope of Regression Line	≥ 0.7 and ≤ 1.3	0.94	1.05	1.07
	Timing of Absolute Maximum Values	Within +/- 10 ms difference: more than 75 %	94.40%	91.70%	97.20%

IV. DISCUSSION

The authors believe that the major points in the development of the SUBP FE model in this study are:

・ *Point 1:* In Step 2.4(a), we successfully identified load conditions of the hip joint that significantly influence the probability of lower limb injuries (important load conditions).

- *Point 2:* In Step 2.4(d), the parameters of each specification of the simplified pelvis FE model were optimized using the "Taguchi Method" to develop the SUBP FE model.

In Point 1, Step 2.4(a), we considered that the differences of output values of injury evaluation items between the simplified pelvis FE model and the human full body FE model are due to the differences in load conditions applied to the hip joint. Therefore, we analyzed the degree of influence of the load conditions for the hip joint (Mx, Fy, and Fx) on the output values of injury evaluation items. The results indicated that the influence of Fy applied to the hip joint is significant for a vehicle with a relatively high vehicle-front shape. On the other hand, Mx and Fz also have influences for a vehicle with a relatively low vehicle-front shape. Those differences can be explained by the following reasons.

- *For collision with a vehicle that has a relatively high vehicle-front shape (e.g., SUV01 and Sedan16):* The vehicle front directly contacts the hip joint region. Fy, which is a force applied to the hip joint in the vehicle longitudinal direction, tends to be large (Figure 15); thus, the influence of Fy is dominant.
- *For collision with a vehicle that has a relatively low vehicle-front shape (e.g., Sedan01):* The vehicle front does not directly contact the hip joint; therefore, Fy, which is a force applied to the hip joint in the vehicle longitudinal direction, does not tend to be as large as that for collisions with a vehicle with a relatively high vehicle-front shape (Figure 16). Therefore, the influence of Fy cannot be dominant.

We successfully identified the load conditions for a hip joint that largely influence the probability of lower limb injuries early in this study; therefore, we could perform subsequent processes for effectively optimizing the simplified pelvis FE model.

It should be noted that, in Figure 7, high values of about 200 Nm were observed for the 100% values of Mx for Sedan16 and Sedan01, because the maximum angles on the adduction side of the hip joint of human full body FE model reach 33 degrees and 32 degrees (the upper limit of the range of motion on the adduction side of an actual human hip joint is 26 to 31 degrees [13]). As a result, the hip joint bottoms out, and relatively high bending moments are observed.

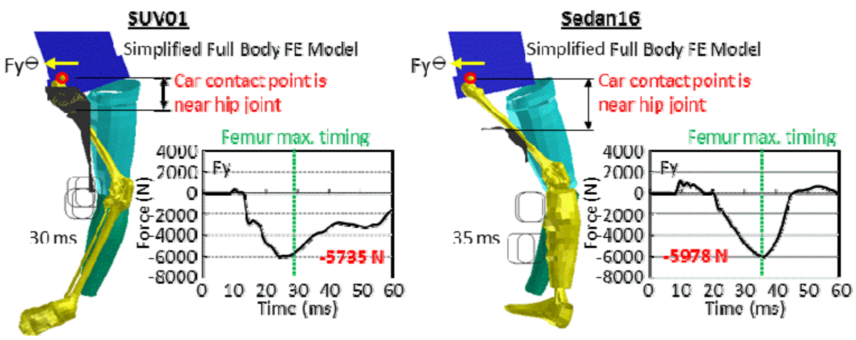

Fig. 15. Fy for Vehicles with a Relatively High Vehicle Front Shape (SUV01 and Sedan16)

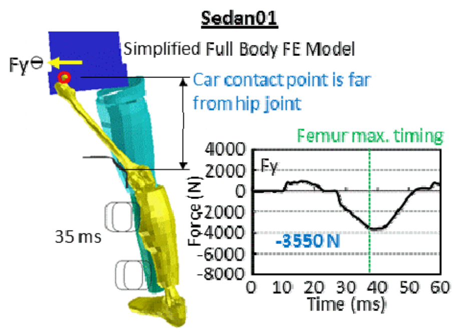

Fig. 16. Fy for Vehicles with a Relatively Low Vehicle Front Shape (Sedan01)

In Point 2, Step 2.4(d), we selected the levels of parameters which maximize the SN ratio using the statistical technique the "Taguchi Method". As a result, the SUBP FE model which has high correlation with the human full body FE model was developed without depending on the intuition or the experience of the analyst.

Based on the graphed factorial effects of the SN ratio (Figure 13), we find that changing the variation levels of mass, COGy and COGz greatly contributed to maintaining equivalency of the output values on injury evaluation items of the SUBP FE model with those of the human full body FE model.

Changing the variation levels of these three parameters generated the following influences, based on the results of sensitivity analysis of each parameter of the specifications for the simplified pelvis FE model implemented in Step 2.4(d).

- *Influence of increasing mass by 3 kg:* Changing mass (Figure 12) resulted in increased bending moment of the lower limb, particularly with collision against a simplified high-bumper vehicle FE model.
- *Influence of moving COGy to the vehicle side by 100 mm:* Changing COGy (Appendix Figure A-10) decreased the bending moment of the lower limb, particularly with collision against a simplified low-medium-bumper vehicle FE model.
- *Influence of moving COGz upward by 50 mm:* Changing COGz (Appendix Figure A-11) decreased the bending moment of the lower limb, particularly with collision against a simplified high-bumper vehicle

FE model and a simplified low-medium-bumper vehicle FE model.

We selected the combination of the optimum variation level using an optimization technique, and the SUBP FE model was developed rationally and efficiently.

V. CONCLUSIONS

In this study, we developed a SUBP model that can appropriately consider the influences of the pedestrian upper body part using CAE analysis methods as well as an optimization technique. As a result, we successfully developed the SUBP FE model that enables appropriate evaluation of the probability of pedestrian lower limb injuries in collisions with any type of vehicle, including high-bumper vehicles.

In our future research, we will apply the SUBP FE model to a flexible pedestrian legform impactor FE model to confirm the SUBP FE model appropriateness to the flexible pedestrian legform impactor FE model. After confirming the appropriateness, we will develop an actual test method (SUBP + flexible pedestrian legform impactor) which can be used in test laboratories worldwide.

VI. REFERENCES

[1] Integrated Project on Advanced Protection Systems (APROSYS). Evaluation of the extended scope for FlexPLI obtained by adding an upper body mass, http://www.aprosys.com/Documents/deliverables/FinalDeliverables.

[2] UN/ECE/WP29/GRSP/INF-GR-PS/Flex-TEG 2008. Design of a Proposed Upper Body Mass (UBM), TEG-065, http://www.unece.org/trans/main/wp29/wp29wgs/wp29grsp/pedestrian_FlexPLI.html.

[3] Isshiki T, Konosu A, Takahashi Y. Investigation of an appropriate pedestrian legform impact test method for vehicles including those with high bumpers (First Report) - Analysis of influence of pedestrian upper body, 2012, *JSAE* No. 100-12, paper no. 20125655.

[4] UN/ ECE/TRANS/180/Add.9, Global Technical Regulation No.9 (Pedestrian safety), http://www.unece.org/trans/main/wp29/wp29wgs/wp29gen/wp29glob_registry.html

[5] Mizuno Y, Chairman, on behalf of IHRA/ P.S. WG. Summary of IHRA Pedestrian Safety WG Activities (2005). Proposed Test Methods to Evaluate Pedestrian Protection Afforded by Passenger Cars, *19th International Technical Conference on the Enhanced Safety of Vehicles*, 2005, paper no. 05-0138.

[6] Takahashi Y, Kikuchi Y, Mori F, Konosu A. Advanced FE lower limb model for pedestrians, *Proceedings of 18th International Technical Conference on the Enhanced Safety of Vehicles*, 2003, paper no. 03-0218.

[7] Takahashi Y, Kikuchi Y, Mori F. Development of a finite element model for a pedestrian pelvis and lower limb, *Society of Automotive Engineers World Congress*, 2006, SAE paper no. 2006-01-0683.

[8] Kikuchi Y, Takahashi Y, Mori F. Full-scale validation of a human FE model for the pelvis and lower limb of a pedestrian, *Society of Automotive Engineers World Congress, 2008,* SAE paper no. 2008-01-1243.

[9] Takahashi Y, Suzuki S, Ikeda M, Gunji Y. Investigation on pedestrian pelvis loading mechanisms using finite element simulations, *Proceedings of IRCOBI Conference,* 2010, Hanover, Germany.

[10] Teresinski, G, Madro, R, Knee joint injuries as a reconstructive factor in car-to-pedestrian accidents, *Forensic Science International, 124, 2001,* pp. 74-82.

[11] UN/ECE/WP29/GRSP/GTR N°9 Phase 2 (GTR9-2)/GTR9-2 7th session /(JASIC) Development of Flex-GTR Master Leg FE Model and Evaluation of Validity of Current Threshold Values, https://www2.unece.org/wiki/download/attachments/11173904/GTR9-7-08e.pdf

[12] Homepage of Robust Quality Engineering Society, http://www.qes.gr.jp/

[13] Asbjørn Roaas and Gunnar B. J. Andersson, Normal Range of Motion of the Hip, Knee and Ankle Joints in Male Subjects, 30–40 Years of Age, Acta Orthopaedica, 1982, Vol. 53, No. 2 , Pages 205-208

VII. APPENDIX

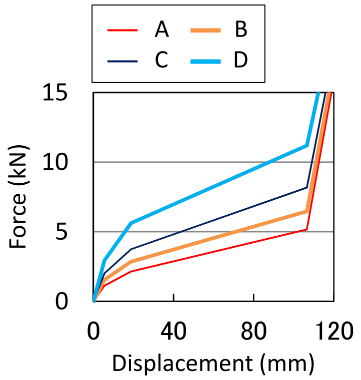

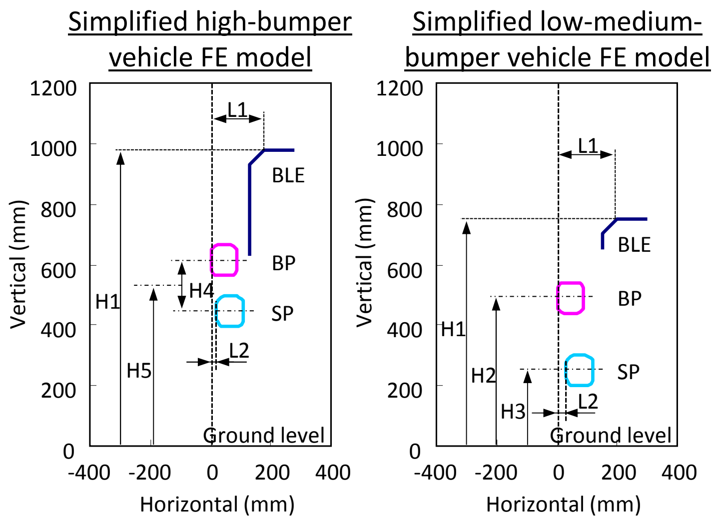

Fig. A-1. Joint Characteristics of BP and SP of the Simplified Vehicle FE Model

Fig. A-2. Parameters of the Vehicle Shape of the Simplified Vehicle FE Model

TABLE A-I

PARAMETERS AND STANDARD LEVELS OF THE SIMPLIFIED VEHICLE FE MODEL

Simplified high-bumper vehicle FE model

Parameter		Unit	Level 1	Level 2	Level 3
K1	(BLE thickness)	mm	0.4	0.6	-
K2	(BP stiffness)	-	B	C	D
K3	(SP stiffness)	-	A	C	D
H1	(BLE height)	mm	900	980	1120
H4	(BP height - SP height)	mm	40	110	170
H5	(Average height of BP and SP)	mm	530	580	670
L1	(BLE lead)	mm	110	180	280
L2	(SP lead)	mm	0	10	20

Simplified low-medium-bumper vehicle FE model

Parameter		Unit	Level 1	Level 2	Level 3
K1	(BLE thickness)	mm	0.4	0.6	-
K2	(BP stiffness)	-	B	C	D
K3	(SP stiffness)	-	A	C	D
H1	(BLE height)	mm	650	700	750
H2	(BP height)	mm	450	490	530
H3	(SP height)	mm	250	270	350
L1	(BLE lead)	mm	125	200	275
L2	(SP lead)	mm	-20	0	30

TABLE A-II

PARAMETERS OF THE SIMPLIFIED VEHICLE FE MODELS FOR 36 VEHICLE TYPES

Simplified High-Bumper Vehicle FE Models									Simplified Low-Medium-Bumper Vehicle FE Models								
ID	K1	K2	K3	H1	H4	H5	L1	L2	ID	K1	K2	K3	H1	H2	H3	L1	L2
SUV01	0.4	B	A	900	40	530	110	0	Sedan01	0.4	B	A	650	450	250	125	-20
SUV02	0.4	B	C	980	110	580	180	10	Sedan02	0.4	B	C	700	490	270	200	0
SUV03	0.4	B	D	1120	170	670	280	20	Sedan03	0.4	B	D	750	530	350	275	30
SUV04	0.4	C	A	900	110	580	280	20	Sedan04	0.4	C	A	650	490	270	275	30
SUV05	0.4	C	C	980	170	670	110	0	Sedan05	0.4	C	C	700	530	350	125	-20
SUV06	0.4	C	D	1120	40	530	180	10	Sedan06	0.4	C	D	750	450	250	200	0
SUV07	0.4	D	A	980	40	670	180	20	Sedan07	0.4	D	A	700	450	350	200	30
SUV08	0.4	D	C	1120	110	530	280	0	Sedan08	0.4	D	C	750	490	250	275	-20
SUV09	0.4	D	D	900	170	580	110	10	Sedan09	0.4	D	D	650	530	270	125	0
SUV10	0.6	B	A	1120	170	580	180	0	Sedan10	0.6	B	A	750	530	270	200	-20
SUV11	0.6	B	C	900	40	670	280	10	Sedan11	0.6	B	C	650	450	350	275	0
SUV12	0.6	B	D	980	110	530	110	20	Sedan12	0.6	B	D	700	490	250	125	30
SUV13	0.6	C	A	980	170	530	280	10	Sedan13	0.6	C	A	700	530	250	275	0
SUV14	0.6	C	C	1120	40	580	110	20	Sedan14	0.6	C	C	750	450	270	125	30
SUV15	0.6	C	D	900	110	670	180	0	Sedan15	0.6	C	D	650	490	350	200	-20
SUV16	0.6	D	A	1120	110	670	110	10	Sedan16	0.6	D	A	750	490	350	125	0
SUV17	0.6	D	C	900	170	530	180	20	Sedan17	0.6	D	C	650	530	250	200	30
SUV18	0.6	D	D	980	40	580	280	0	Sedan18	0.6	D	D	700	450	270	275	-20

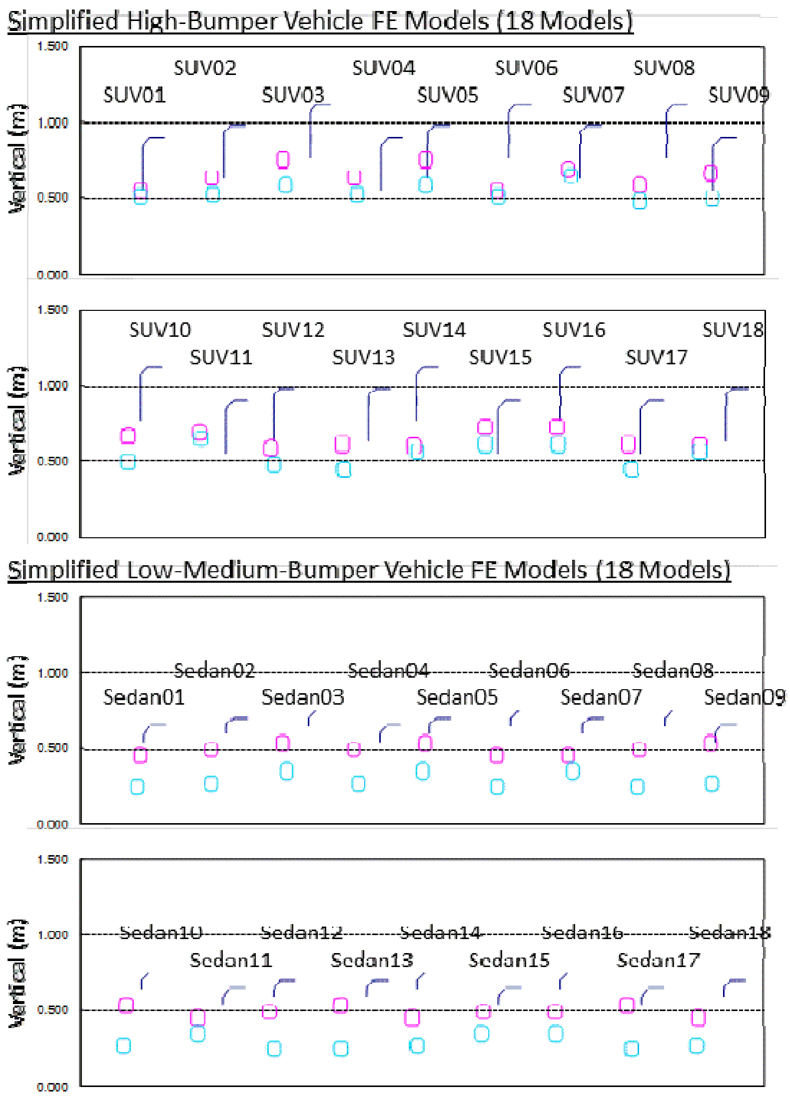

Fig. A-3. Shapes of the Simplified Vehicle FE Models for 36 Vehicle Types

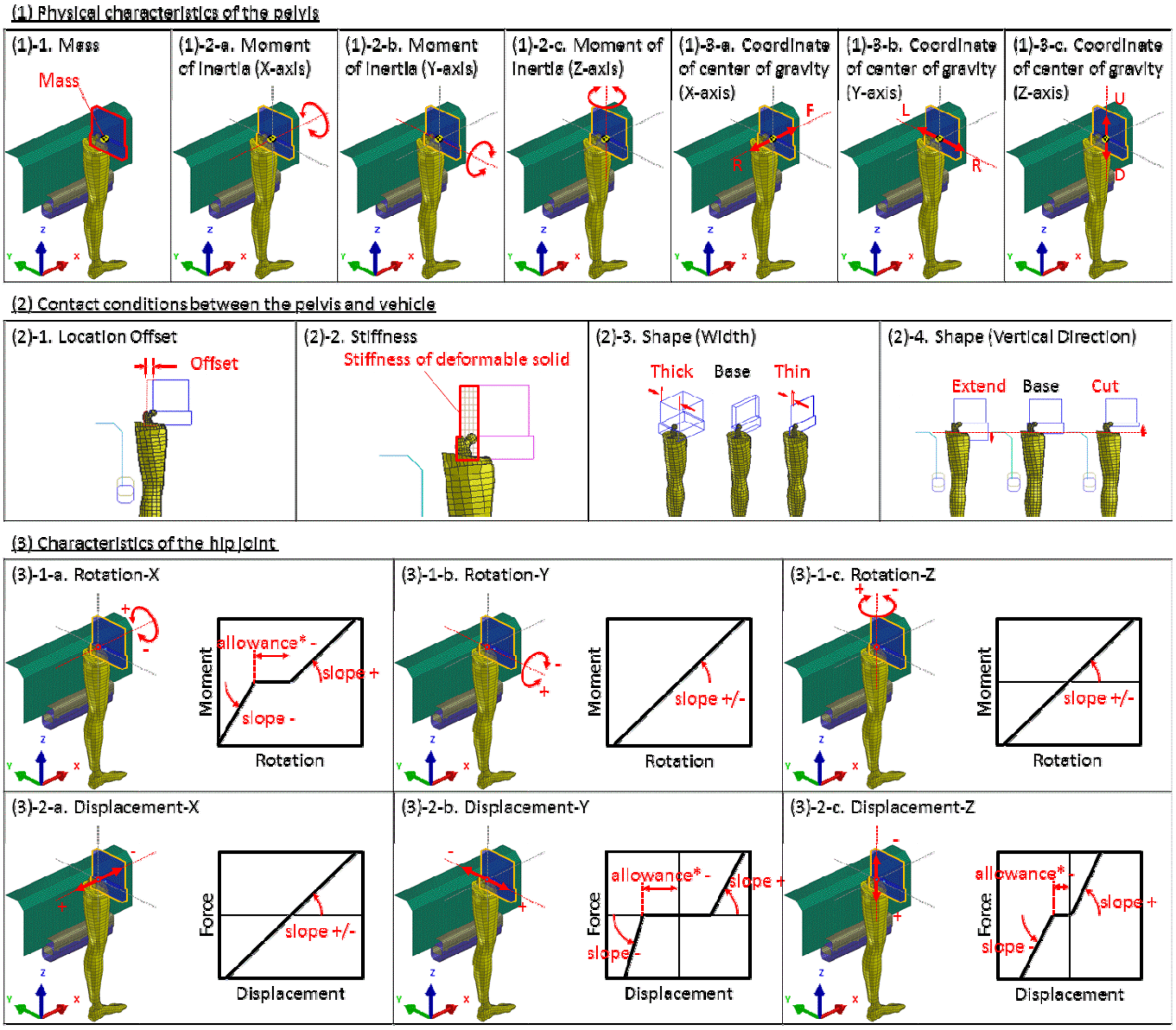

* Allowance: The range of free rotation or free displacement of the hip joint.

Fig. A-4. Parameters of each Specification for the Simplified Pelvis FE Model Subjected to Sensitivity Analysis

TABLE A-III

SIMPLIFIED PELVIS FE MODELS OF 36 SPECIFICATIONS FOR OPTIMIZATION

Modal ID	Parameter												
	P1	P2	P3	P4	P5	P6	P7	P8	P9	P10	P11	P12	P13
	Mass	Ix	COGy	COGz	Offset	Rx(-)a	Rx(-)s	Dy(-)a	Dy(-)s	-	Dz(-)a	Dz(-)s	Dz(+)s
Model01	13.1 kg	x1	L 100 mm	U 50 mm	0 mm	0 deg.	x0.1	0 mm	x0.5	-	0 mm	x0.5	x0.1
Model02	13.1 kg	x2	0 mm	0 mm	-20 mm	10 deg.	x1	5 mm	x1	-	25 mm	x1	x1
Model03	13.1 kg	x5	R 200 mm	D 23 mm	-40 mm	20 deg.	x1.5	10 mm	x100	-	50 mm	x2	x100
Model04	13.1 kg	x1	L 100 mm	U 50 mm	0 mm	10 deg.	x1	5 mm	x1	-	50 mm	x2	x100
Model05	13.1 kg	x2	0 mm	0 mm	-20 mm	20 deg.	x1.5	10 mm	x100	-	0 mm	x0.5	x0.1
Model06	13.1 kg	x5	R 200 mm	D 23 mm	-40 mm	0 deg.	x0.1	0 mm	x0.5	-	25 mm	x1	x1
Model07	13.1 kg	x1	L 100 mm	0 mm	-40 mm	0 deg.	x1	10 mm	x100	-	25 mm	x1	x100
Model08	13.1 kg	x2	0 mm	D 23 mm	0 mm	10 deg.	x1.5	0 mm	x0.5	-	50 mm	x2	x0.1
Model09	13.1 kg	x5	R 200 mm	U 50 mm	-20 mm	20 deg.	x0.1	5 mm	x1	-	0 mm	x0.5	x1
Model10	13.1 kg	x1	L 100 mm	D 23 mm	-20 mm	0 deg.	x1.5	5 mm	x100	-	0 mm	x2	x1
Model11	13.1 kg	x2	0 mm	U 50 mm	-40 mm	10 deg.	x0.1	10 mm	x0.5	-	25 mm	x0.5	x100
Model12	13.1 kg	x5	R 200 mm	0 mm	0 mm	20 deg.	x1	0 mm	x1	-	50 mm	x1	x0.1
Model13	16.1 kg	x1	0 mm	D 23 mm	0 mm	20 deg.	x1	0 mm	x100	-	25 mm	x0.5	x1
Model14	16.1 kg	x2	R 200 mm	U 50 mm	-20 mm	0 deg.	x1.5	5 mm	x0.5	-	50 mm	x1	x100
Model15	16.1 kg	x5	L 100 mm	0 mm	-40 mm	10 deg.	x0.1	10 mm	x1	-	0 mm	x2	x0.1
Model16	16.1 kg	x1	0 mm	D 23 mm	-20 mm	0 deg.	x0.1	10 mm	x1	-	50 mm	x1	x0.1
Model17	16.1 kg	x2	R 200 mm	U 50 mm	-40 mm	10 deg.	x1	0 mm	x100	-	0 mm	x2	x1
Model18	16.1 kg	x5	L 100 mm	0 mm	0 mm	20 deg.	x1.5	5 mm	x0.5	-	25 mm	x0.5	x100
Model19	16.1 kg	x1	0 mm	U 50 mm	-40 mm	20 deg.	x1.5	0 mm	x1	-	0 mm	x1	x100
Model20	16.1 kg	x2	R 200 mm	0 mm	0 mm	0 deg.	x0.1	5 mm	x100	-	25 mm	x2	x0.1
Model21	16.1 kg	x5	L 100 mm	D 23 mm	-20 mm	10 deg.	x1	10 mm	x0.5	-	50 mm	x0.5	x1
Model22	16.1 kg	x1	0 mm	0 mm	-40 mm	20 deg.	x0.1	5 mm	x0.5	-	50 mm	x2	x1
Model23	16.1 kg	x2	R 200 mm	D 23 mm	0 mm	0 deg.	x1	10 mm	x1	-	0 mm	x0.5	x100
Model24	16.1 kg	x5	L 100 mm	U 50 mm	-20 mm	10 deg.	x1.5	0 mm	x100	-	25 mm	x1	x0.1
Model25	19.1 kg	x1	R 200 mm	0 mm	0 mm	10 deg.	x1.5	10 mm	x0.5	-	0 mm	x1	x1
Model26	19.1 kg	x2	L 100 mm	D 23 mm	-20 mm	20 deg.	x0.1	0 mm	x1	-	25 mm	x2	x100
Model27	19.1 kg	x5	0 mm	U 50 mm	-40 mm	0 deg.	x1	5 mm	x100	-	50 mm	x0.5	x0.1
Model28	19.1 kg	x1	R 200 mm	0 mm	-20 mm	10 deg.	x0.1	0 mm	x100	-	50 mm	x0.5	x100
Model29	19.1 kg	x2	L 100 mm	D 23 mm	-40 mm	20 deg.	x1	5 mm	x0.5	-	0 mm	x1	x0.1
Model30	19.1 kg	x5	0 mm	U 50 mm	0 mm	0 deg.	x1.5	10 mm	x1	-	25 mm	x2	x1
Model31	19.1 kg	x1	R 200 mm	D 23 mm	-40 mm	10 deg.	x1.5	5 mm	x1	-	25 mm	x0.5	x0.1
Model32	19.1 kg	x2	L 100 mm	U 50 mm	0 mm	20 deg.	x0.1	10 mm	x100	-	50 mm	x1	x1
Model33	19.1 kg	x5	0 mm	0 mm	-20 mm	0 deg.	x1	0 mm	x0.5	-	0 mm	x2	x100
Model34	19.1 kg	x1	R 200 mm	U 50 mm	-20 mm	20 deg.	x1	10 mm	x0.5	-	25 mm	x2	x0.1
Model35	19.1 kg	x2	L 100 mm	0m m	-40 mm	0 deg.	x1.5	0 mm	x1	-	50 mm	x0.5	x1
Model36	19.1 kg	x5	0 mm	D 23 mm	0 mm	10 deg.	x0.1	5 mm	x100	-	0 mm	x1	x100

Model_ID	Integrated values ($x10^{-3}$ Nm・s)												SN ratio (dB)
	SUV01						Sedan01						
	Femur-3		Femur-2		Femur-1		Femur-3		Femur-2		Femur-1		
	+ side	- side	+ side	- side	+ side	- side	+ side	- side	+ side	- side	+ side	- side	
	N1	N2	N3	N4	N5	N6	N7	N8	N9	N10	N11	N12	
Model01	2728.0	-2250.1	1683.9	-2120.9	1151.7	-2036.9	4358.3	-71.3	3339.3	-74.1	2092.1	-49.5	-66.9
Model02	927.3	-5495.9	817.5	-4608.3	575.6	-3077.2	1941.7	-123.6	2124.2	-92.7	1834.7	-49.1	-68.2
:	:	:	:	:	:	:	:	:	:	:	:	:	:
Model36	2498.7	-2895.6	1920.9	-1990.0	1294.2	-891.6	5623.3	-63.4	4436.6	-72.0	2819.3	-46.2	-68.1

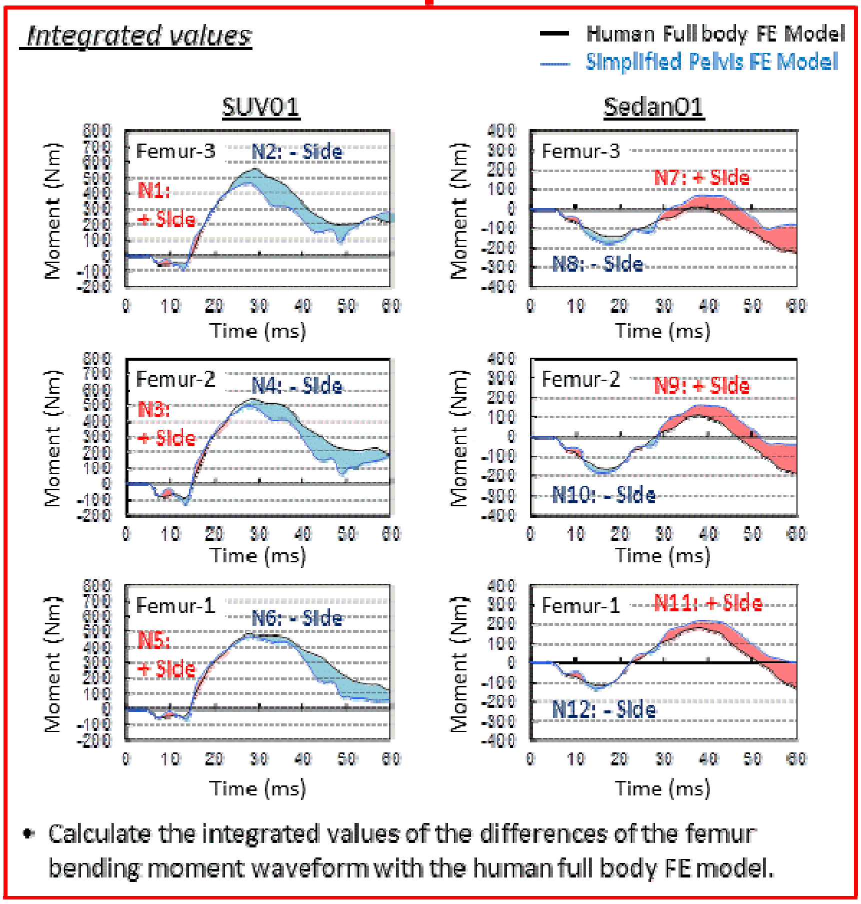

Signal noise ratio (SN ratio)

- Calculate the Signal Noise ratio (SN ratio) using the calculated integrated values.

Fig. A-5. Example of calculated integrated values and SN ratio values

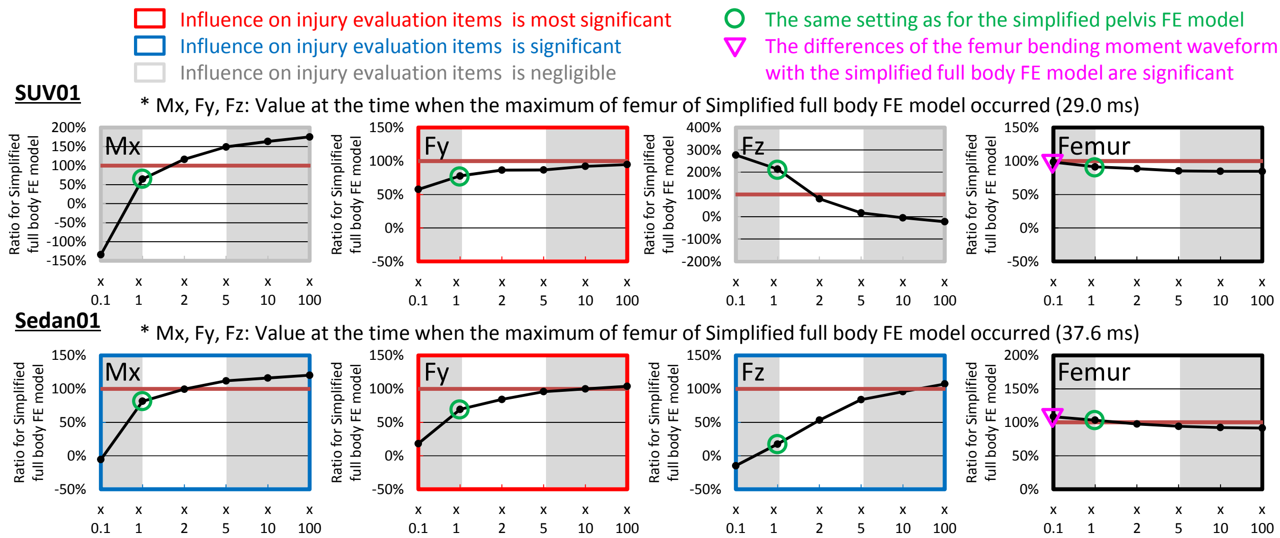

Fig. A-6. Results of Sensitivity Analysis of the Simplified Pelvis FE Model (Ix)

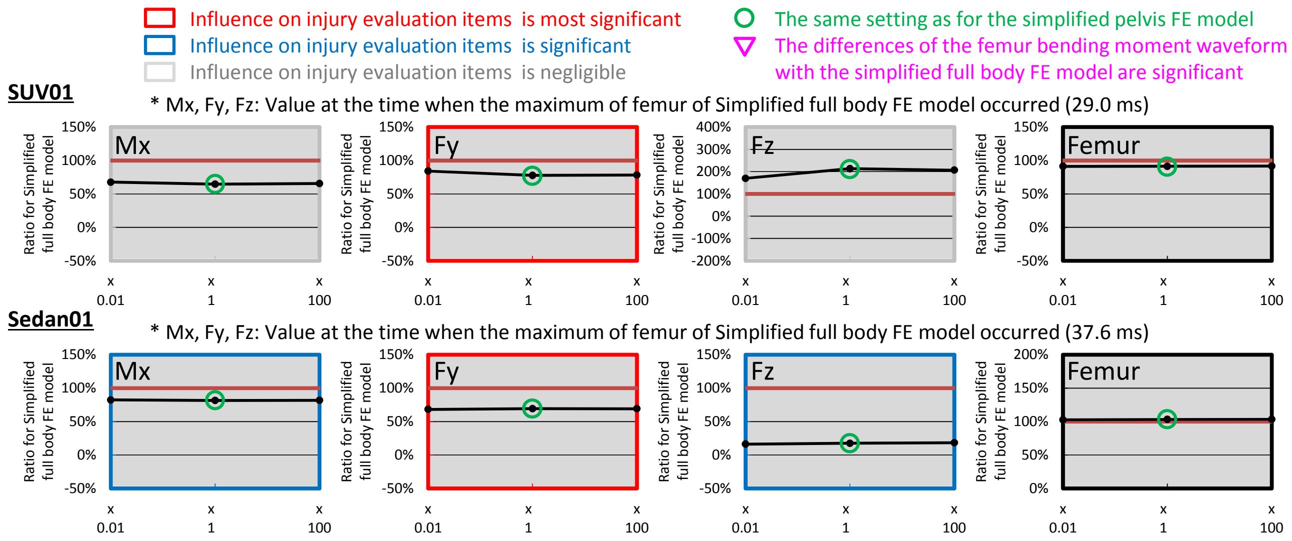

Fig. A-7. Results of Sensitivity Analysis of the Simplified Pelvis FE Model (Iy)

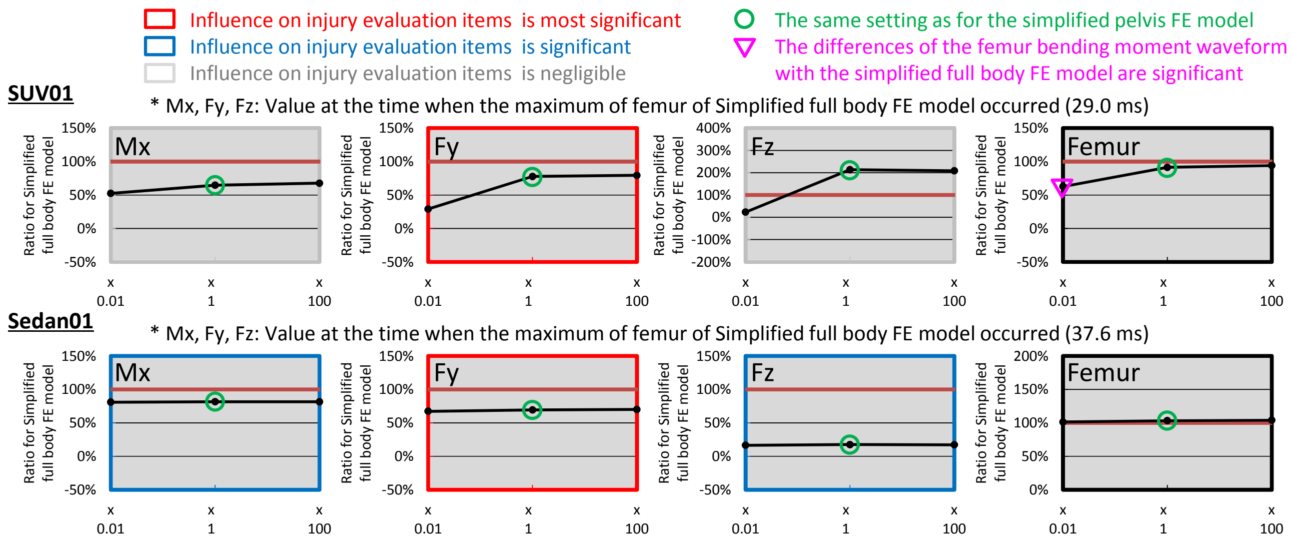

Fig. A-8. Results of Sensitivity Analysis of the Simplified Pelvis FE Model (Iz)

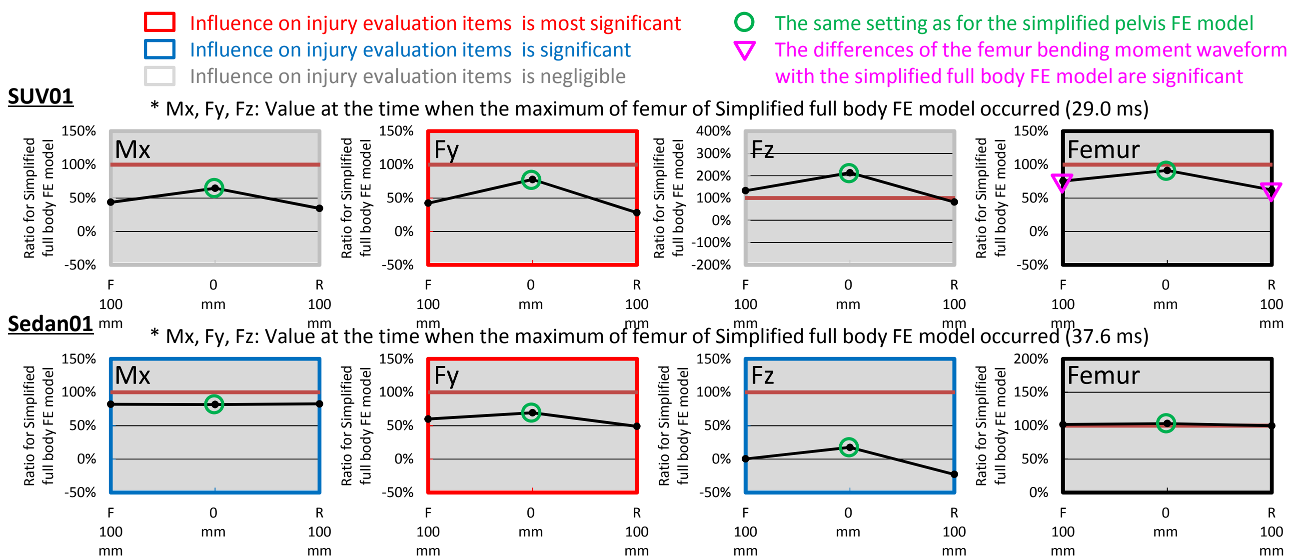

Fig. A-9. Results of Sensitivity Analysis of the Simplified Pelvis FE Model (COGx)

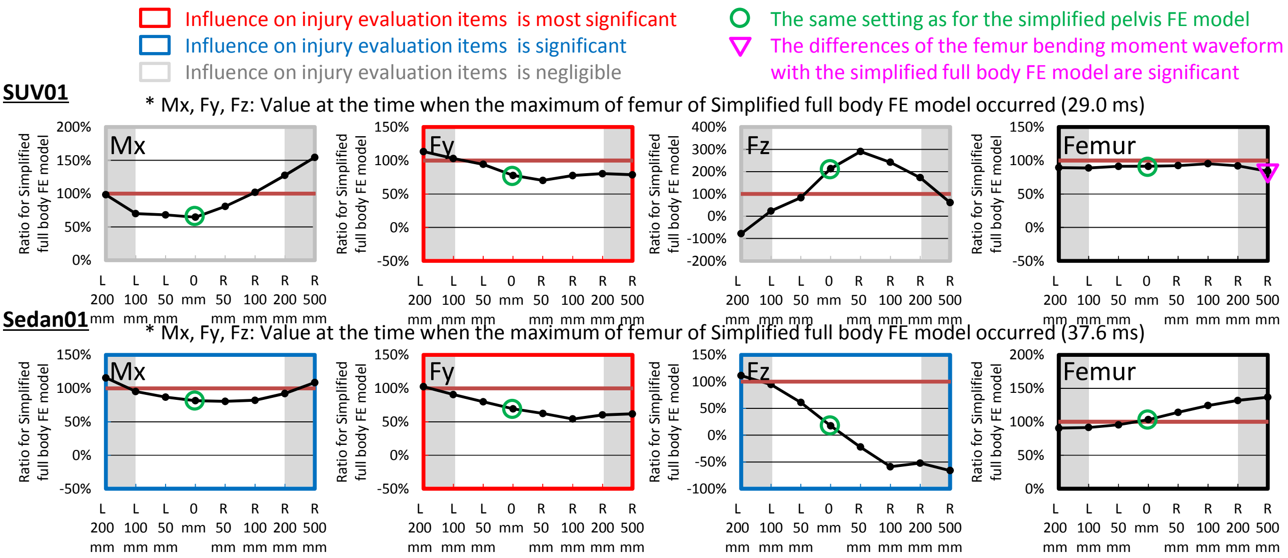

Fig. A-10. Results of Sensitivity Analysis of the Simplified Pelvis FE Model (COGy)

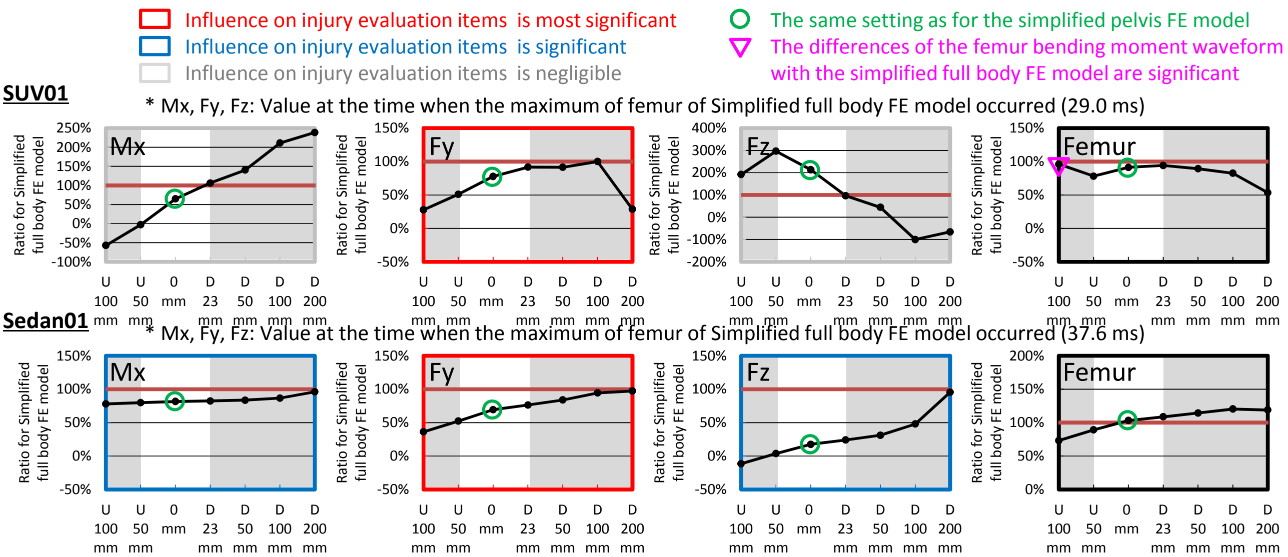

Fig. A-11. Results of Sensitivity Analysis of the Simplified Pelvis FE Model (COGz)

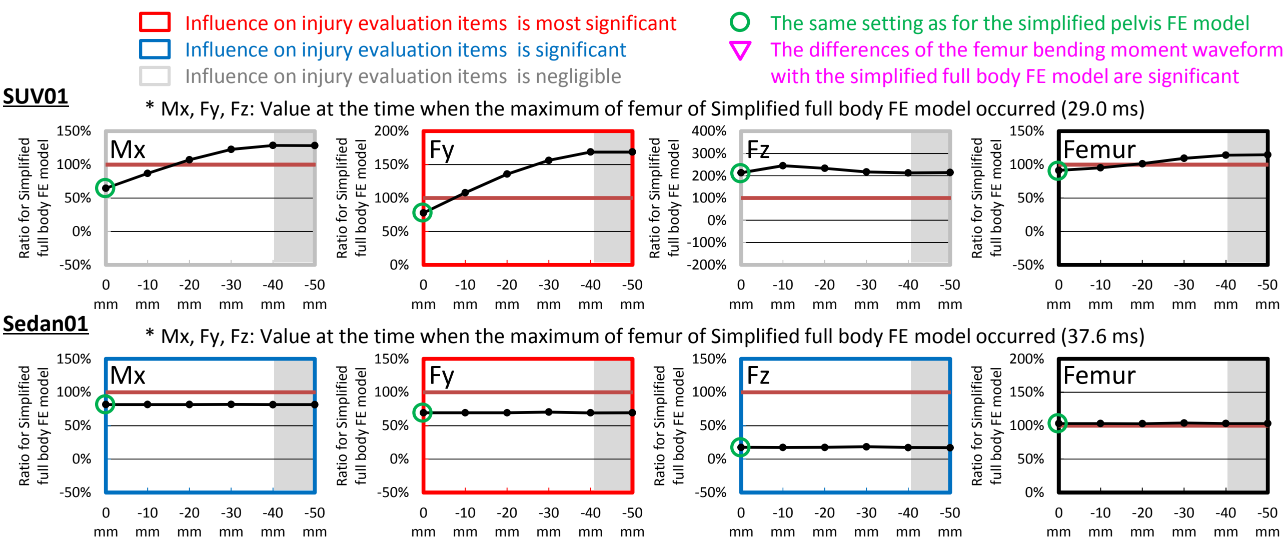

Fig. A-12. Results of Sensitivity Analysis of the Simplified Pelvis FE Model (offset)

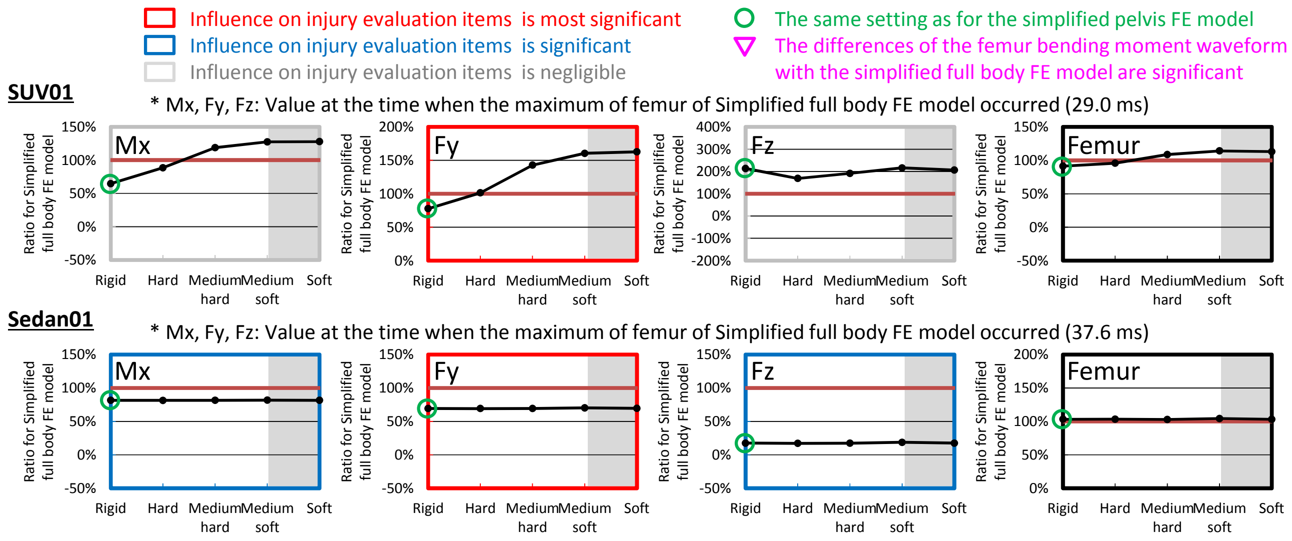

Fig. A-13. Results of Sensitivity Analysis of the Simplified Pelvis FE Model (stiffness)

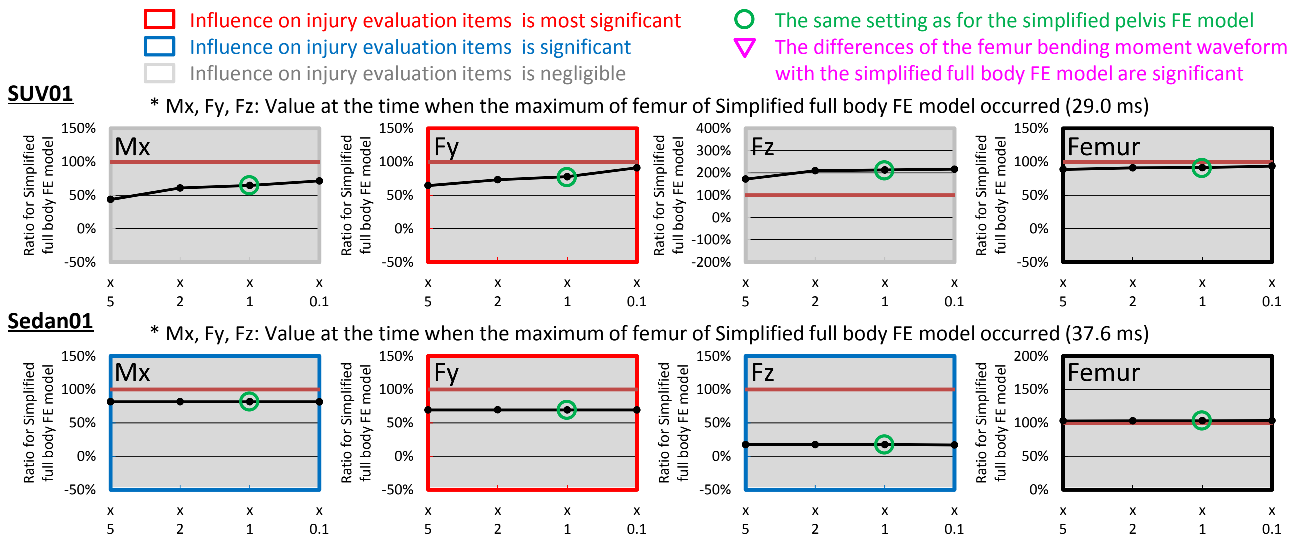

Fig. A-14. Results of Sensitivity Analysis of the Simplified Pelvis FE Model (shape thickness)

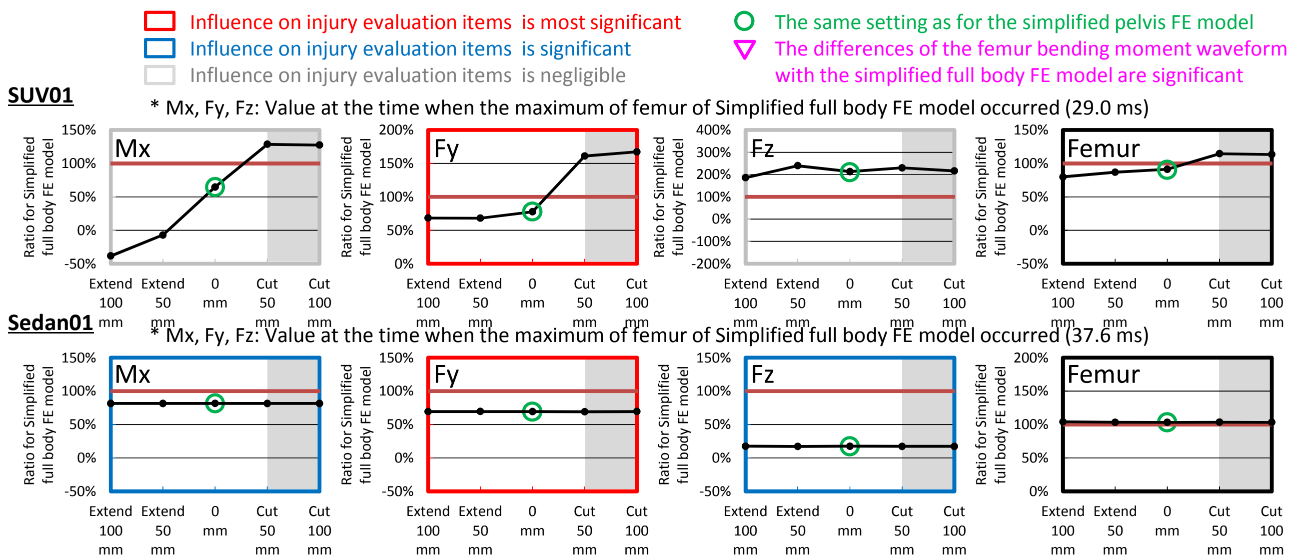

Fig. A-15. Results of Sensitivity Analysis of the Simplified Pelvis FE Model (shape vertical)

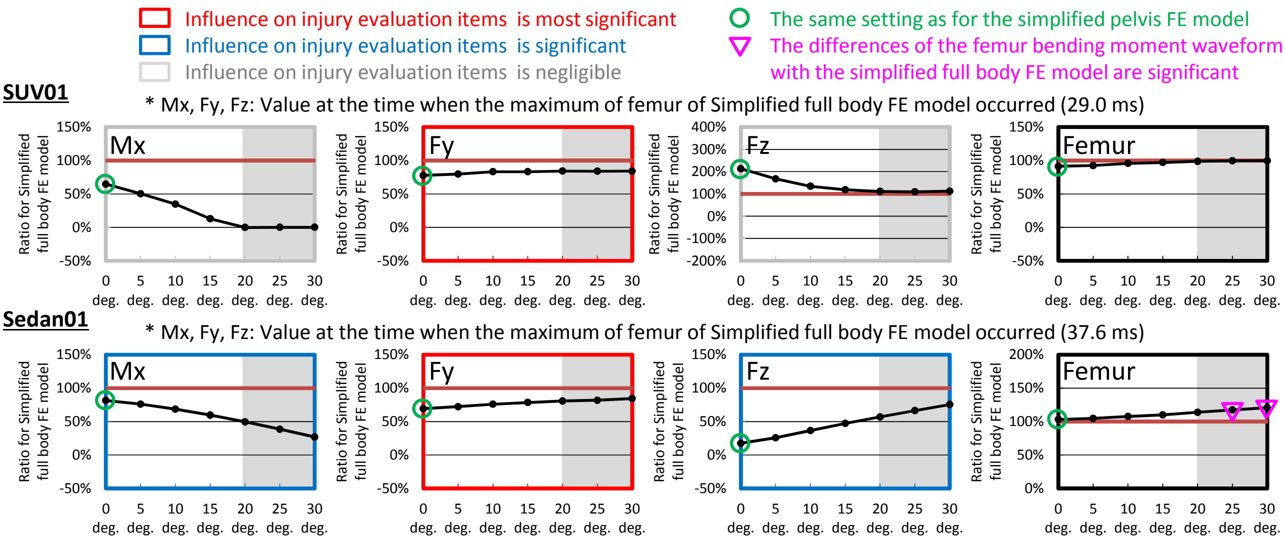

Fig. A-16. Results of Sensitivity Analysis of the Simplified Pelvis FE Model (Rx(-)a)

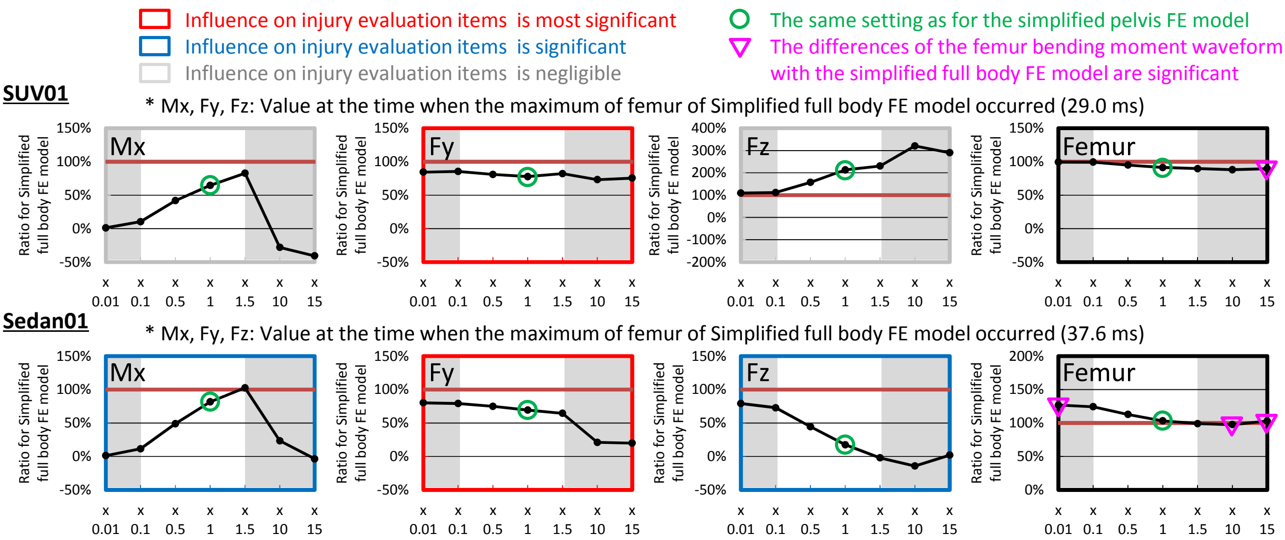

Fig. A-17. Results of Sensitivity Analysis of the Simplified Pelvis FE Model (Rx(-)s)

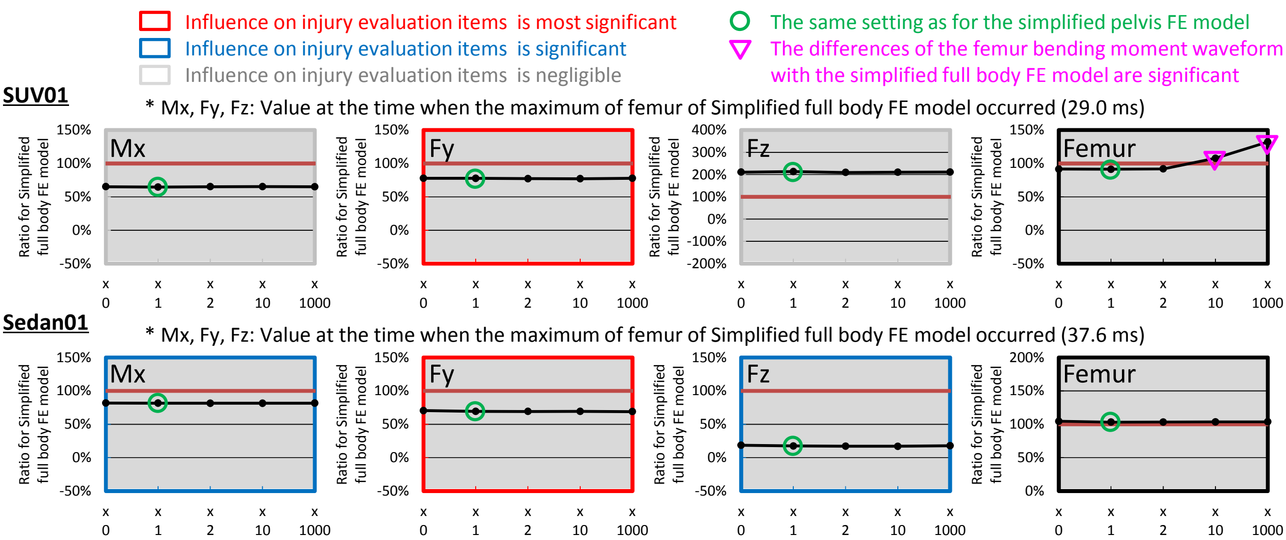

Fig. A-18. Results of Sensitivity Analysis of the Simplified Pelvis FE Model (Rx(+)s)

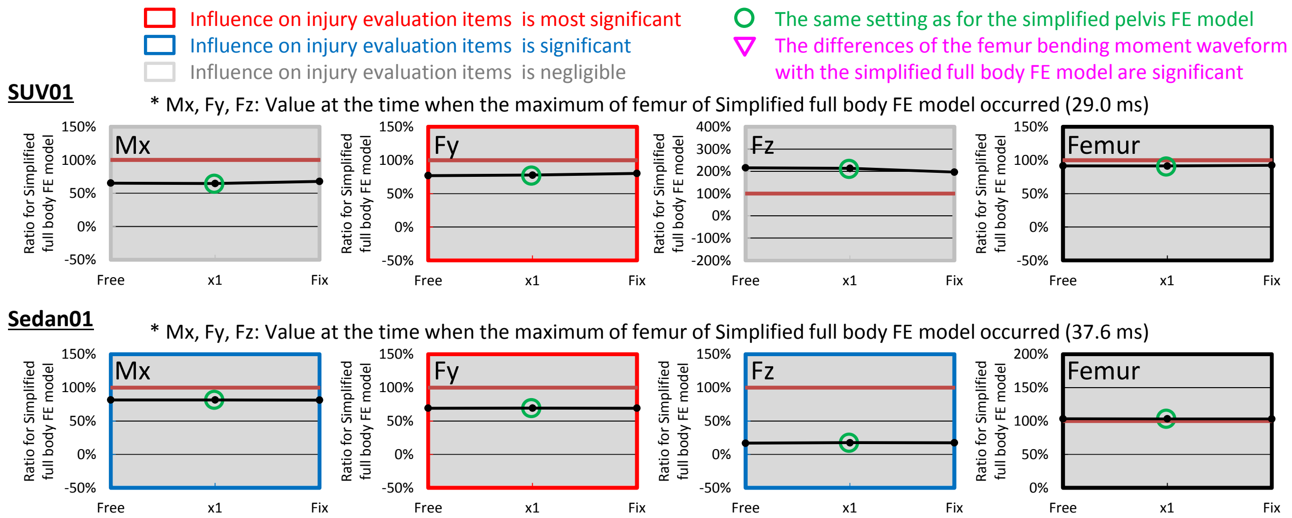

Fig. A-19. Results of Sensitivity Analysis of the Simplified Pelvis FE Model (Ry(+/-)s)

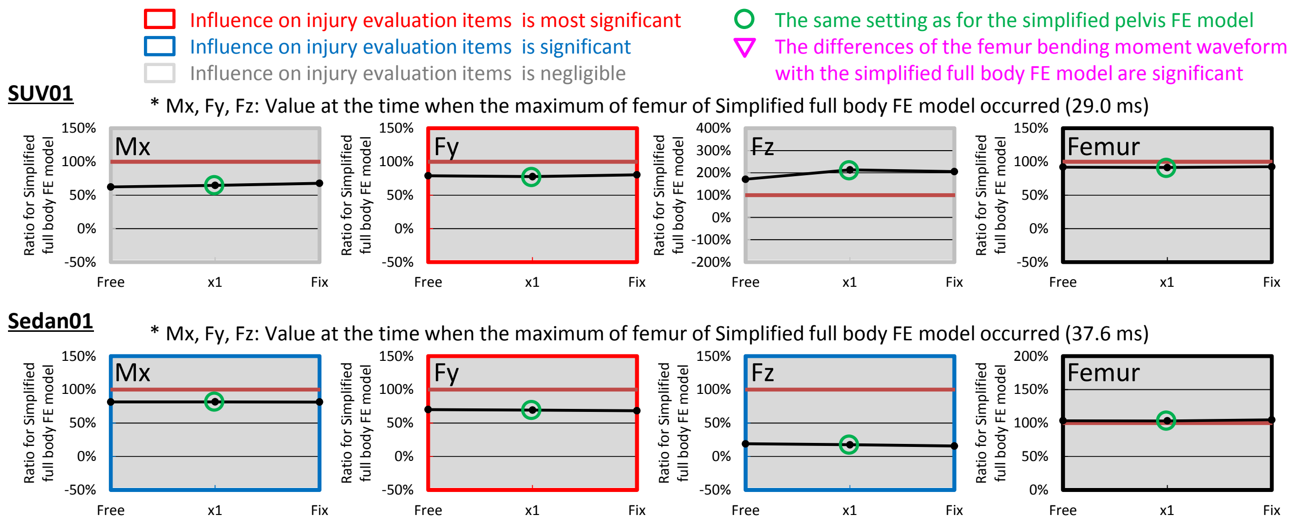

Fig. A-20. Results of Sensitivity Analysis of the Simplified Pelvis FE Model (Rz(+/-)s)

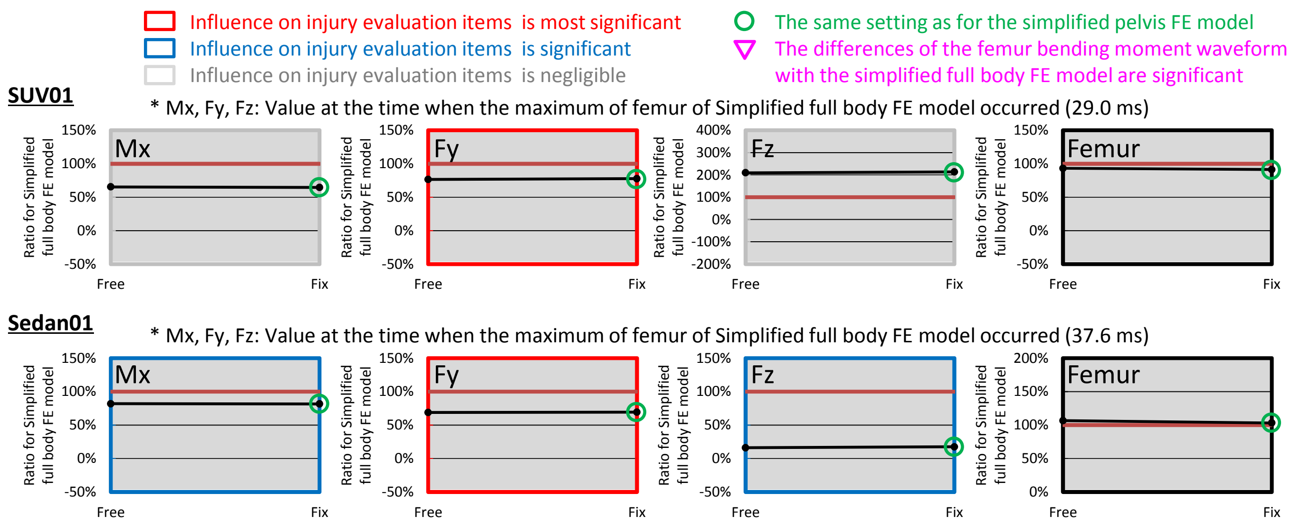

Fig. A-21. Results of Sensitivity Analysis of the Simplified Pelvis FE Model (Dx(+/-)s)

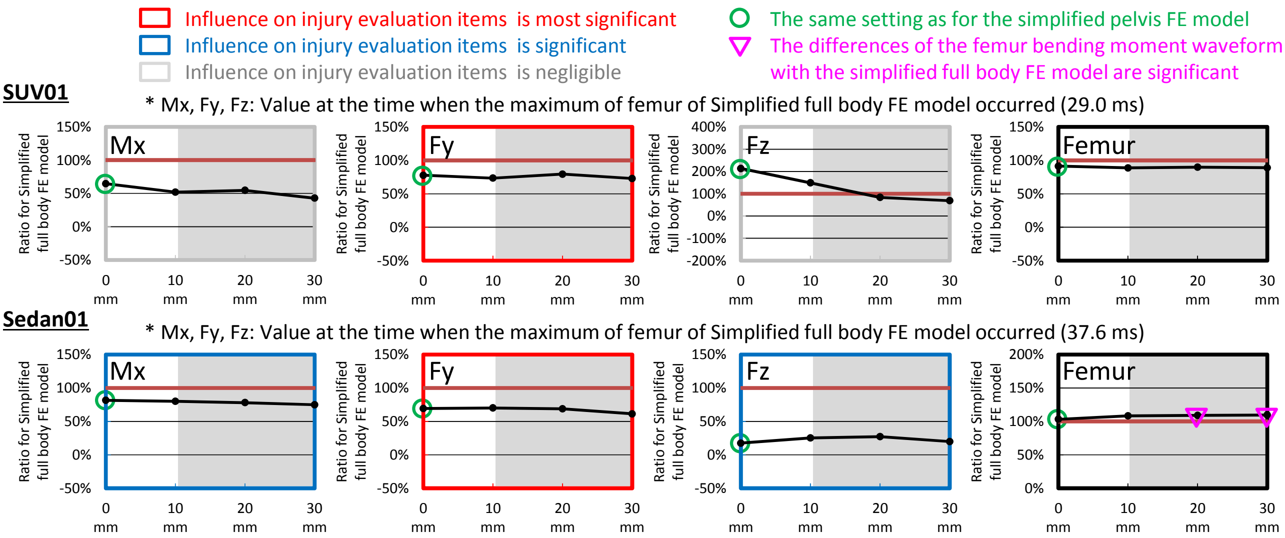

Fig. A-22. Results of Sensitivity Analysis of the Simplified Pelvis FE Model (Dy(-)a)

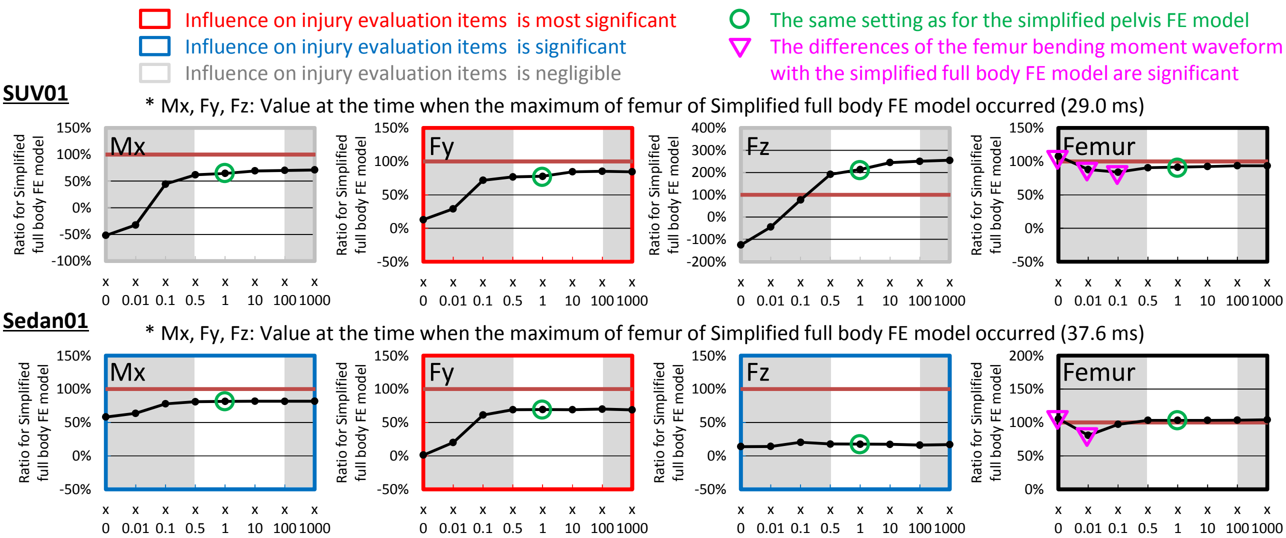

Fig. A-23. Results of Sensitivity Analysis of the Simplified Pelvis FE Model (Dy(-)s)

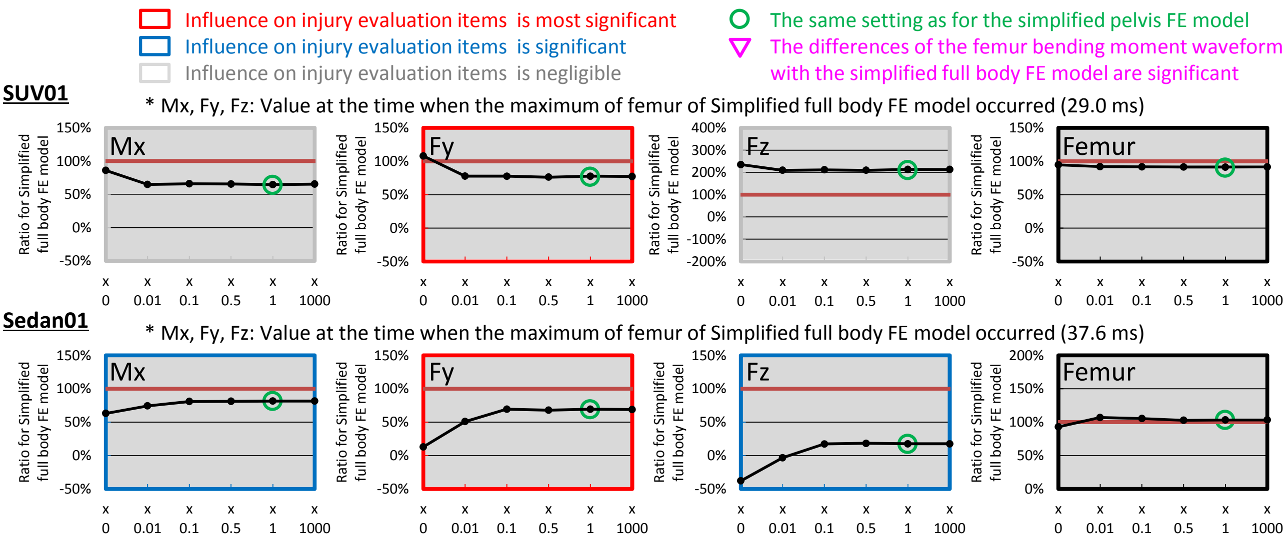

Fig. A-24. Results of Sensitivity Analysis of the Simplified Pelvis FE Model (Dy(+)s)

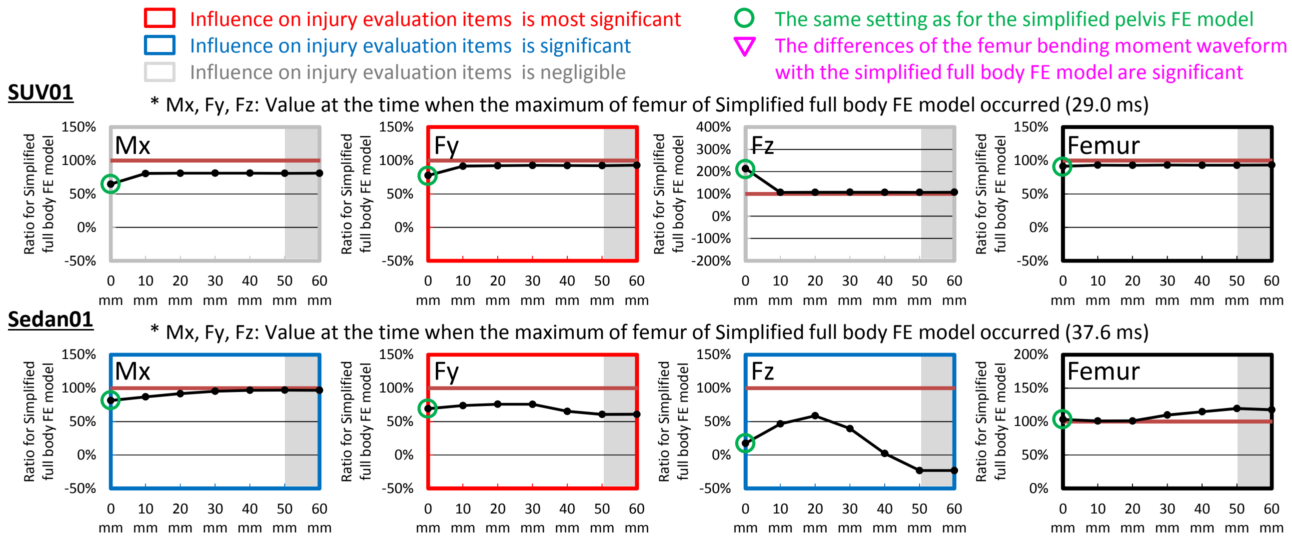

Fig. A-25. Results of Sensitivity Analysis of the Simplified Pelvis FE Model (Dz(-)a)

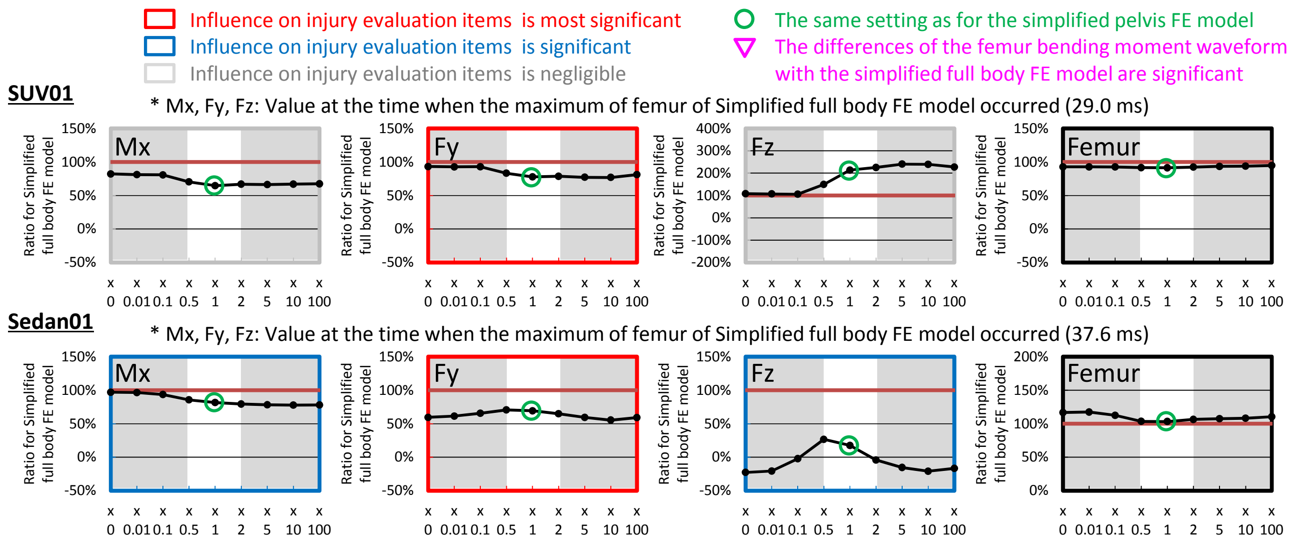

Fig. A-26. Results of Sensitivity Analysis of the Simplified Pelvis FE Model (Dz(-)s)

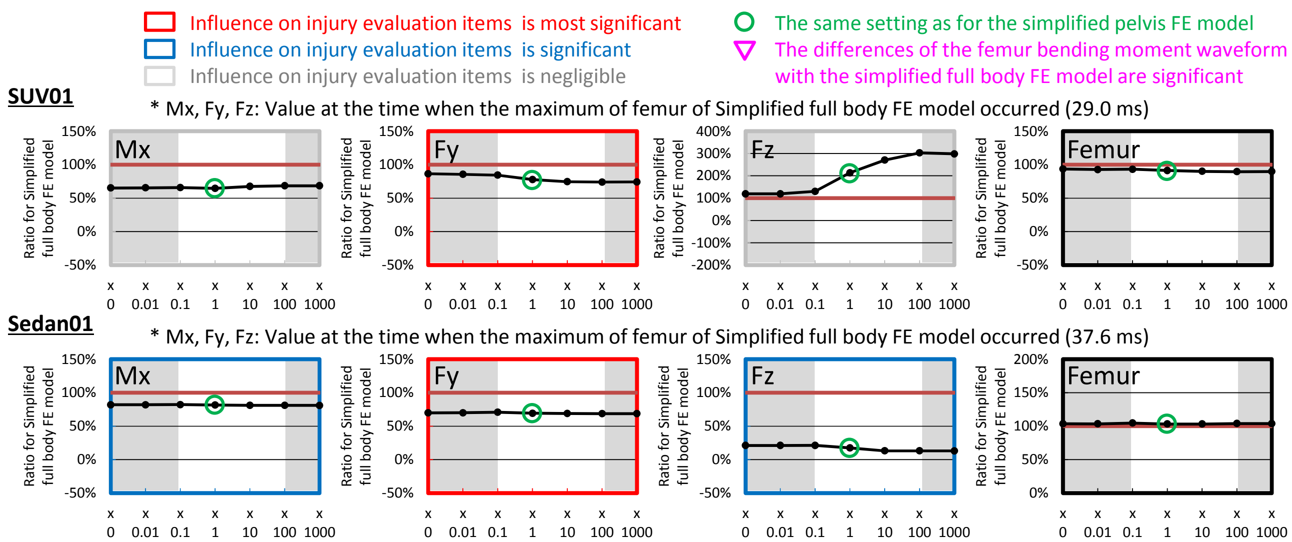

Fig. A-27. Results of Sensitivity Analysis of the Simplified Pelvis FE Model (Dz(+)s)

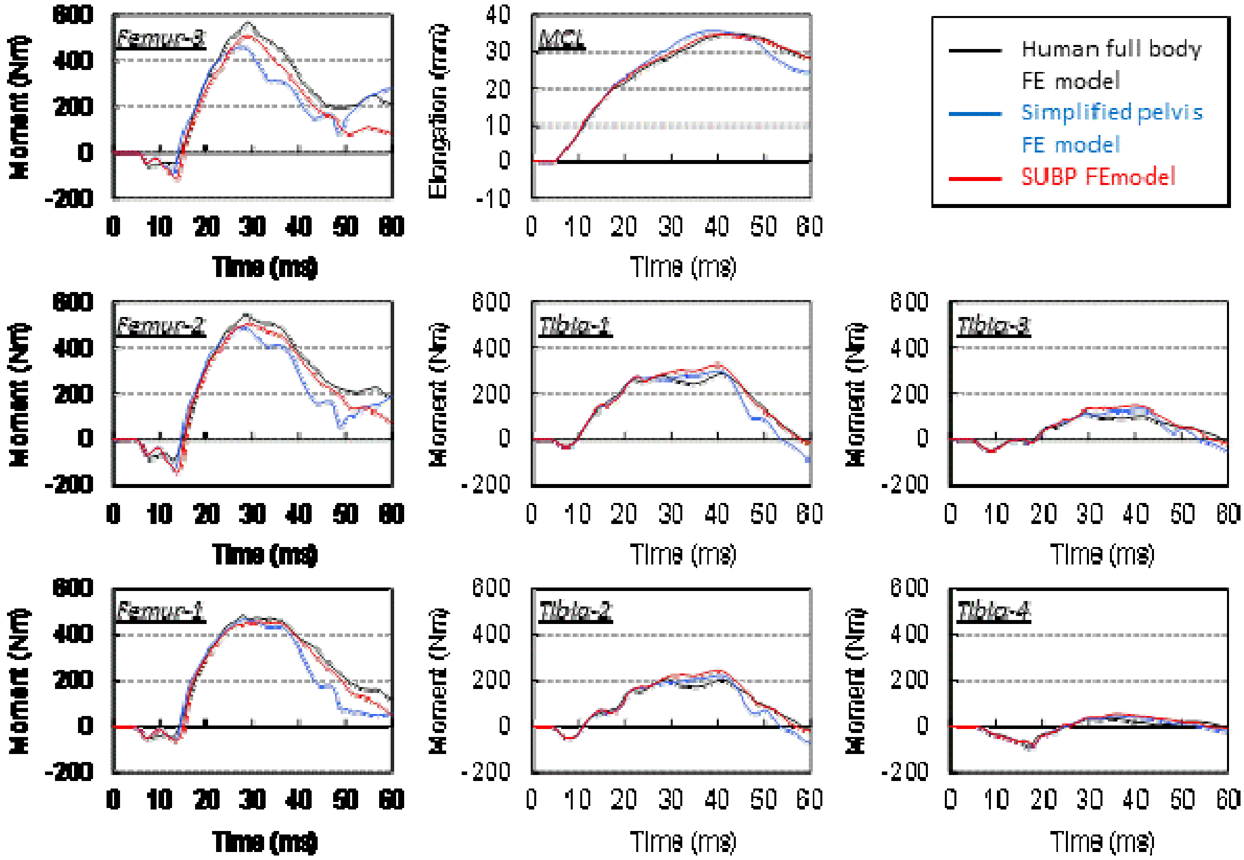

Fig. A-28. Waveform of the SUBP FE Model (SUV01)

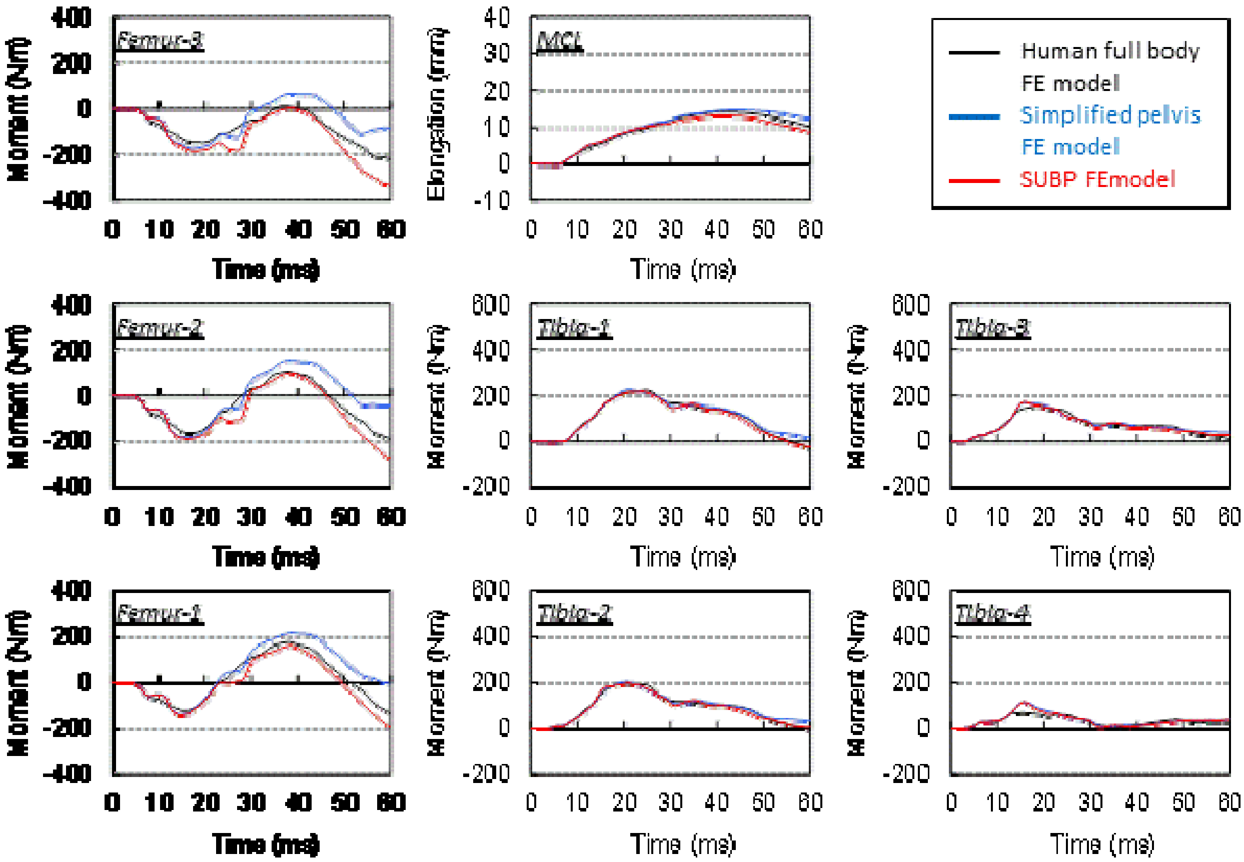

Fig. A-29. Waveform of the SUBP FE Model (Sedan01)